In presenting the dissertation as a partial fulfillment of the requirements for an advanced degree from the Georgia Institute of Technology, I agree that the Library of the Institute shall make it available for inspection and circulation in accordance with its regulations governing materials of this type. I agree that permission to copy from, or to publish from, this dissertation may be granted by the professor under whose direction it was written, or, in his absence, by the Dean of the Graduate Division when such copying or publication is solely for scholarly purposes and does not involve potential financial gain. It is understood that any copying from, or publication of, this dissertation which involves potential financial gain will not be allowed without written permission.

3/17/65
b

REFLECTANCE ERRORS OF THE MODIFIED INTEGRATING SPHERE REFLECTOMETER

A THESIS

Presented to

The Faculty of the Graduate Division

by

Sung Hwan Cho

In Partial Fulfillment

of the Requirements for the Degree

Master of Science in Mechanical Engineering

Georgia Institute of Technology

September, 1966

REFLECTANCE ERRORS

OF THE MODIFIED INTEGRATING SPHERE REFLECTOMETER

Approved:

Chairman

Date approved by chairman 9/12/66

ACKNOWLEDGMENTS

The author is indebted to a number of persons who have helped and encouraged him in this endeavor. Primarily, he wishes to thank Dr. R. C. Birkebak, without whose careful instruction and advice this thesis would not have been completed. The services of Dr. J. E. Sunderland and Dr. C.W. Gorton, who served on the reading committee, are also appreciated.

The author wishes to thank Mr. H. U. Hwang and Mr. C. T. Kwon for their encouragement and suggestions.

Thanks are also due to the Korean Military Academy, which has supported his study in the United States.

The partial support from NASA Grant No. G-657 and the loan of the integrating sphere radiometer by the Aerospace Environmental Facility of Arnold Engineering Development Center (AEDC), Air Force Systems Command (AFSC) are gratefully acknowledged.

Finally, the author expresses his personal gratitude to his uncle and teacher, Mr. Suk Ki Cho, whose guidance, encouragement, and support have been invaluable to him.

TABLE OF CONTENTS

LIST OF TABLES

LIST OF ILLUSTRATIONS

SUMMARY

An experimental study of blockage effects of center mounted samples in a modified integrating sphere reflectometer was conducted.

For a diffusely reflecting sample surface, the irradiance on the sphere wall in the upper hemisphere has nearly a cosine distribution, while in the lower hemisphere it is uniform. For a specularly reflecting sample surface, the irradiance on the sphere wall is uniform except for small areas caused by the first specular reflection from the sample.

A review of the theory for the modified integrating sphere reflectometer was made. This resulted in the derivation of a new set of equations for the wall irradiance in the upper and the lower hemispheres, as well as for the equations to calculate the reflectance of a center mounted sample.

For the absolute measurement of reflectances, errors are introduced by the center mounted test sample. These errors are a function of sample size, reflectances of both front and back surfaces of the test sample, and detector location.

For relative measurement of reflectances, i.e., comparison of the test sample to a surface of known reflectance, errors will be introduced if back surfaces of different reflectances are used.

NOMENCLATURE

English Letters		Typical Units
A	total area of the interior sphere wall	ft^2
A_d	area of the detector	ft^2
A_s	area of the test sample	ft^2
E_o	incident energy into the sphere	watt
k	detector constant	mv/watt
R	radius of the sphere (= 7 inches)	inch
r	radius of the test sample	inch
V_o	detector response at $\phi = 90^o$ without sample	mv
V_r	detector response when reference surface is illuminated at θ	mv
V_s	detector response when test sample is illuminated at θ	mv
V_{sh}	detector response at first reflection shaded area when sphere wall is illuminated at Ψ	mv
$V^l_{\theta,\phi}$	detector response at ϕ (lower hemisphere) when sample is illuminated at θ	mv
$V^u_{\theta,\phi}$	detector response at ϕ (upper hemisphere) when sample is illuminated at θ	mv
$V_{\Psi,\theta}$	detector response at ϕ when sphere wall is illuminated at Ψ	mv
Greek Letters		
ρ_s	reflectance of test sample	dimensionless

ρ_r	reflectance of reference surface	dimensionless
ρ_{s_1}	reflectance of the front surface of the test sample	dimensionless
ρ_{s_2}	reflectance of the back surface of the test sample	dimensionless
ρ_w	reflectance of the sphere wall	dimensionless
ρ_w'	"apparent" reflectance of the sphere wall	dimensionless
θ	angle of incidence of illumination on the test sample or reference surfaces	deg
ϕ	polar angle of reflection	deg
Ψ	polar angle of incident illumination on the sphere wall	deg

CHAPTER I

INTRODUCTION

In the measurement of thermal radiation properties, accuracy is of prime importance if the results are to be useful in radiation heat transfer calculations. Maximum relative errors in calculated equilibrium temperatures of one-fourth of those of the radiation properties used are possible in given circumstances. The accuracy of radiation property measurements depends on the radiometric technique used. Of interest in this thesis is the use of one specific radiometer, the modified integrating sphere used to measure reflectance values in the visible region of the spectrum.

Dunkle[1] has compared various methods to measure reflectances; Coblentz integrating hemisphere, Gier-Dunkle heated hohlraum, and the integrating sphere reflectometer. He concluded that the integrating sphere method was the best for the reflectance measurement in the visible wave length region, if a careful choice of sphere wall material, suitable positions of detector, sample, and entrance port were made.

In the classical integrating sphere the sample, reference surface, and detector are placed on the sphere wall surface[1-6]. If all the surfaces are perfectly diffuse reflectors, the irradiance on the wall is uniform since the shape factor between any two area elements on the sphere wall is constant.

For the measurements of angular-hemispherical or hemispherical-angular reflectances, a simple modification can be made to the integrating

sphere. In the modified integrating sphere a test sample is placed at the center of the sphere so that by turning the sample the reflectance can be obtained for various angle of incidence[7-10]. Figure 1 shows schematic diagrams of the classical and modified integrating spheres.

Errors in the integrating sphere method are caused by many factors. In the classical integrating sphere, the main errors are caused by[1-11]

(1) Finite sizes of the entrance port, sample, and detector area,

(2) Imperfectly diffuse reflectance of the sphere wall,

(3) Specular reflectance of the test sample,

(4) Polarization of the light source.

Hardy and Pineo[7] have analyzed the errors caused by finite sizes of the entrance port and sample. Jacquez and Kuppenheim[3,4] analyzed the theory of the classical integrating sphere for a perfect sphere with perfectly diffuse or specular samples, and for spheres with flat samples and reference surfaces. Hisdal[5] has analyzed the theory of the integrating sphere for the case of a finite flat non-perfectly diffuse sample using form factors and finite difference equations. Recently, Zerlaut and Krupnick[19] have measured the reflectances by comparing with a black body and report large errors for non-perfectly diffuse samples. All investigators assumed perfectly diffuse reflecting sphere walls and non-polarized light sources.

Brandenberg[20] has studied a modified integrating sphere for hemispherical-angular reflectance measurements. He has analyzed errors caused by imperfectly diffuse reflectance of sample surface, polarization of light beam, and exit port.

In the modified integrating sphere, another error is introduced.

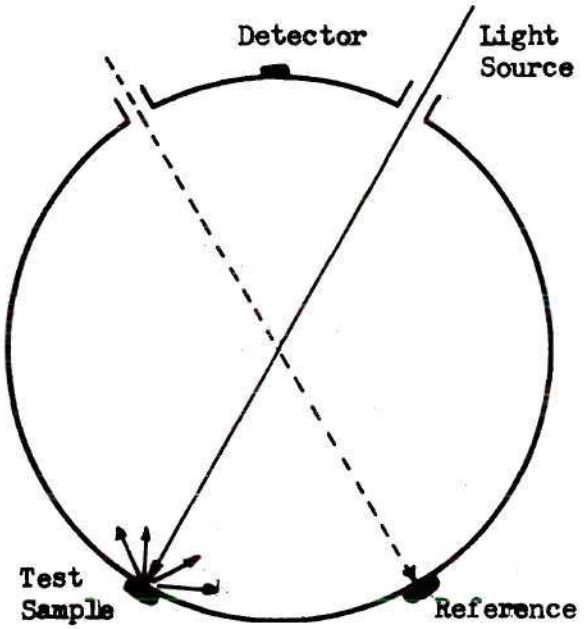

Classical Integrating Sphere

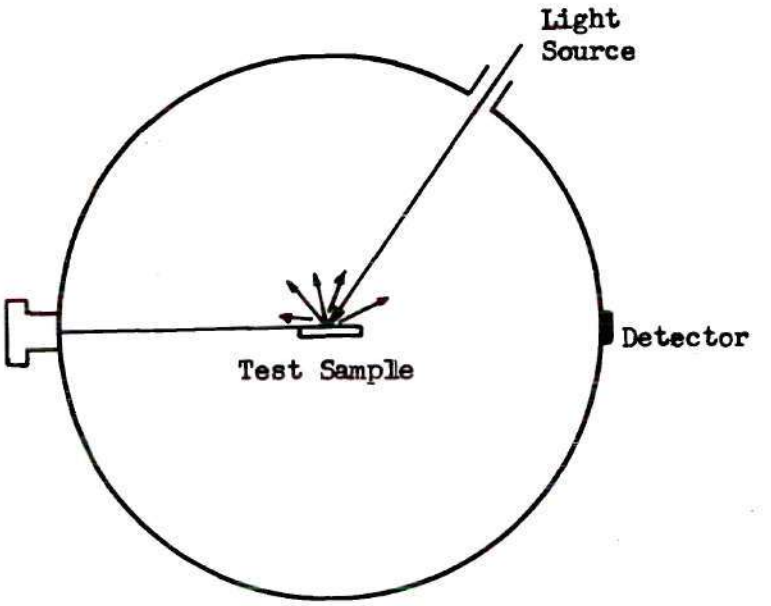

Modified Integrating Sphere

Figure 1. Schematic Diagrams of Integrating Spheres

The irradiance on the sphere wall is not uniform because of the blockage caused by the centrally located test sample even though the sphere wall and sample surfaces are perfectly diffuse reflectors. This effect has been neglected by previous investigators. Eberhart[8] analyzed both the classical and modified integrating spheres, but he assumed uniform sphere wall irradiance. Edwards, et al.[9], analyzed the modified integrating sphere for imperfectly diffuse samples but also neglected sample blockage effects. Dawson, et al.[12], have analyzed the modified integrating sphere and have calculated the errors in reflectance measurement caused by centrally located sample with various sphere to sample radius ratios, sample reflectances, specular component of the sample reflectance, incident angles, and detector locations using a numerical computing technique.

The present work is an experimental study of the blockage effects of a centrally located sample on the measurement of reflectance in the modified integrating sphere. The experiment was carried out for various sphere to sample radius ratios, reflectances of front and back surfaces of the test sample, and detector locations.

CHAPTER II

APPARATUS

The experimental apparatus used in this study consisted very simply of a modified integrating sphere, various sizes of test samples, and associated detecting and recording equipment.

Integrating Sphere

The integrating sphere used in this study was a modification of a commercially available integrating sphere radiometer (Heatransfer Laboratories, Inc. Model No. IRS-1A). The apparatus consisted of an aluminum sphere, 7 inches ID, a tungsten-iodine light source, a light collimating tube, a sensor attached to a rotatable arm, sample holder, and a magnesium oxide (MgO) coating on the interior wall. Details are shown in Fig. 2.

The collimating tube was constructed so that it could be tilted for illuminating either the sample or sphere wall. The collimating tube was smoked black inside and the diameter of the entrance aperture is 0.115 inches.

A solar cell of size 1 x 2 centimeters was used as a detector. The detector holder is located at right angles to the collimating tube and in the same plane as the sample holder. The distance between the sphere wall and the detector surface is approximately 3/16 inches. The detector arm can be rotated so that one diametral plane of the sphere can be mapped for intensity variations with the detector.

The sample holder is located at right angles to the collimating tube

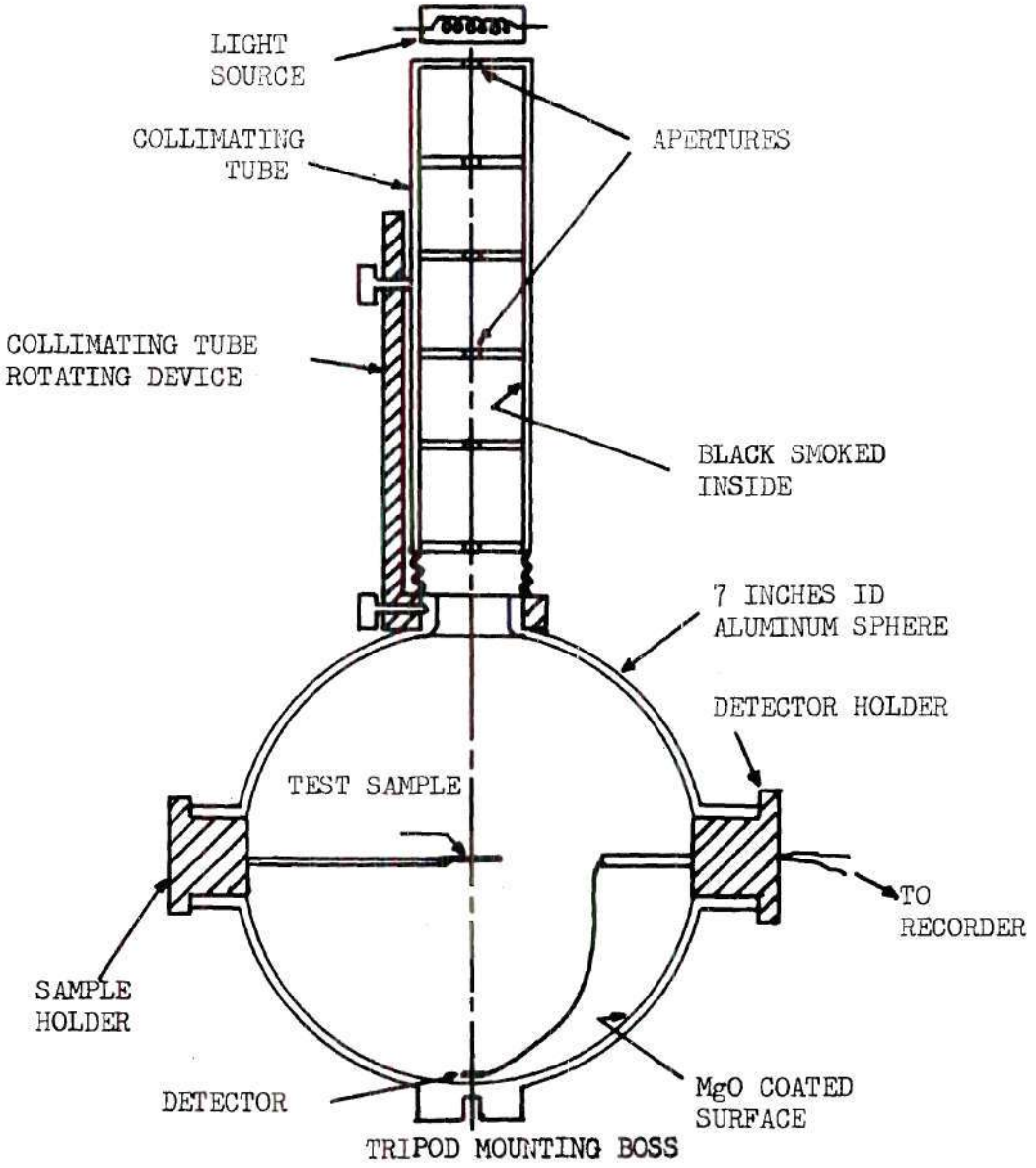

Figure 2. Modified Integrating Sphere Reflectometer

and is a polished copper rod, MgO coated, 1/8 inch in diameter, to which samples can be attached. The sample holder can be rotated for any desired angle of incidence of light on the sample.

The light source is a 6.5 ampere, 30 volt tungsten-iodine lamp, the characteristics of which are obtained from Arnold Engineering Development Center and are shown in Fig. 3. The light source is surrounded with blackened cover to eliminate any scattered energy from entering the sphere.

Recorder

A strip chart recorder (Moseley Model 7100 BM Strip Chart Recorder with Plug-in Model 17501A Input Module) was used. Its accuracy is better than 0.2 per cent of full scale. The range of the input module is from 1 millivolt to 100 volts full scale recording.

Test Samples

The test samples were constructed from a commercial aluminum plate of 0.0175 inch thickness. The sample surfaces are MgO coated, carbon blackened (acetylene soot), or polished aluminum. The thickness of MgO coating was approximately 1 millimeter. The machine polished aluminum surfaces are quite specular reflecting, though their perfectness cannot be claimed.

The abbreviation $\frac{\text{MgO}}{\text{Al}}$ indicates a test sample with MgO coated front surface and its back surface is polished aluminum. Also, $\frac{\text{Black}}{\text{MgO}}$ indicates a test sample with carbon blackened front surface and MgO coated back surface.

The diameters of the test samples used were 0.7, 1.0, 1.4, and

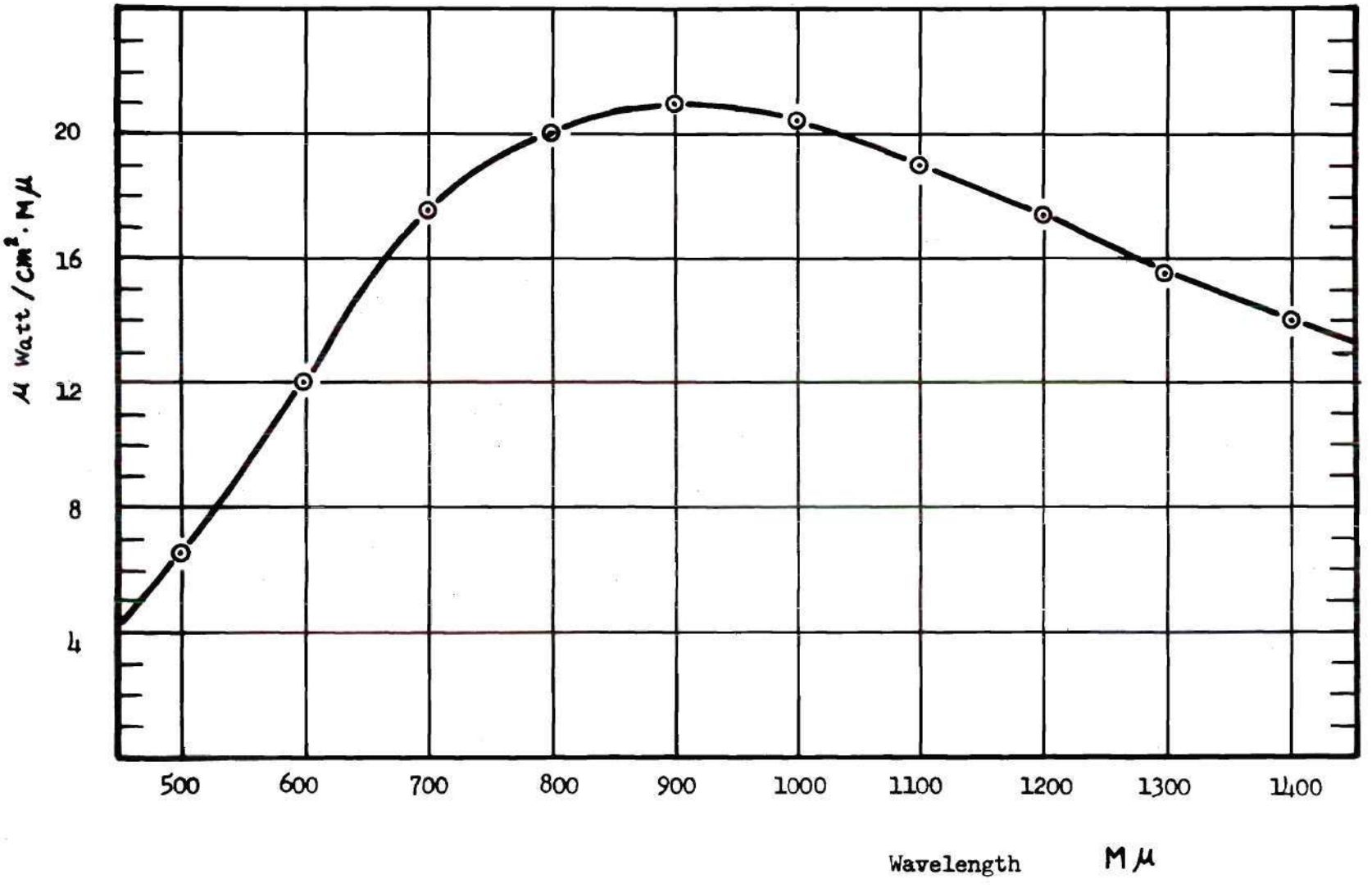

Figure 3. Wavelength Distribution for Tungsten-Iodine Lamp

1.75 inches, so that the sphere to sample radius ratios, R/r, are 10, 7, 5, and 4, respectively.

CHAPTER III

EXPERIMENTAL PROCEDURE

The detector linearity was checked with a set of neutral density filters (Optics Technology, Inc., Set No. 12), and found to be linear within 2 per cent in the range shown in Fig. 4.

The intensity of the light source was fixed throughout the whole experiment at 200 watts. The collimating tube hole was adjusted so that no light could directly hit the sphere wall when the smallest sample was illuminated. The aperture size remained fixed throughout the experiment. The diameters of the six apertures in the collimating tube were 0.115 inches and the tube was 9 inches long. The diameter of the directly illuminated area on the wall was approximately 3/8 inches, with diffraction and geometric factors of the collimating tube causing some spreading of the light beam.

The diffuseness of the sphere wall was checked several times during the study without the center mounted sample inside the sphere. The detector arm was rotated through 360 deg and the detector output recorded as a function of the detector position. Two positions of illumination on the sphere wall by the light source were used, Ψ = 0 deg and Ψ = 37 deg.

A test sample was put at the center of the sphere and set for the desired angle of incidence of illumination. By adjusting the collimating tube angle, either the sample or the sphere wall could be illuminated with the test sample at the center of the sphere. Measurements were then made

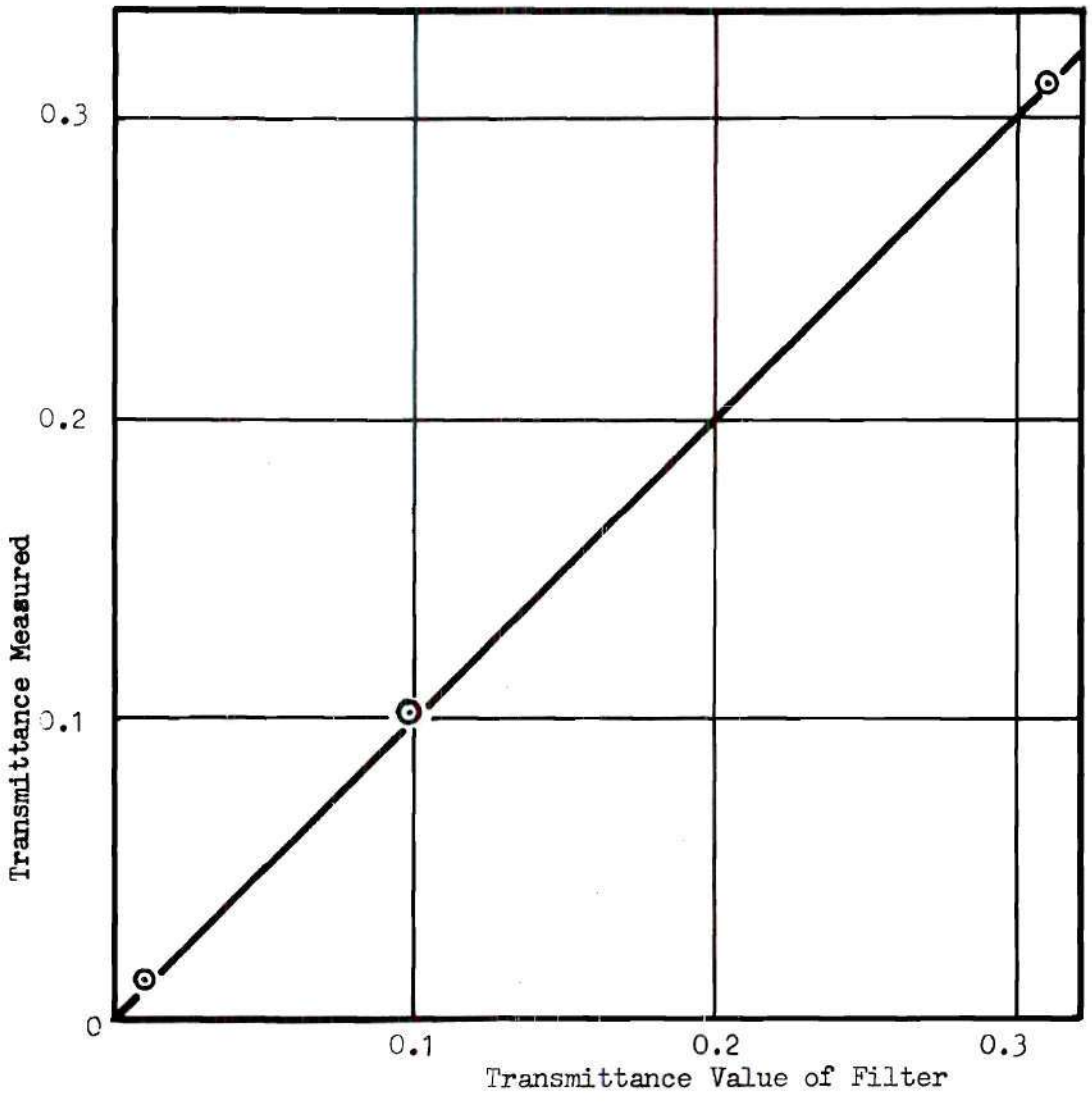

Figure 4. Detector Linearity

for the irradiance on the sphere wall as a function of detector position for either sample or wall illumination.

CHAPTER IV

RESULTS AND DISCUSSIONS

Diffuseness of the Sphere Wall

The integrating sphere theory indicates that if light passes through an aperture into a spherical enclosure whose wall is perfectly diffuse reflecting, the irradiance on the sphere wall is uniform regardless of position. A check of this was made to determine whether the sphere used in this study worked properly. The irradiance $V_{\Psi,\phi}$ of the wall, when the wall is illuminated directly without the sample inside the sphere, is shown in Figs. 5 and 6. The results are normalized by the irradiance of the wall at ϕ = 90 deg. The figures show the uniform irradiance on the wall, except near ϕ = 0 deg (Fig. 5) and ϕ = 354 deg (Fig. 6) where the detector blocks the incident energy, and near ϕ = 180 deg (Fig. 5) and ϕ = 217 deg (Fig. 6) where the detector is directly illuminated. The decrease of detected irradiance close to the directly illuminated area is the result of the detector being displaced 3/16 inches from the sphere wall and therefore it cannot receive any of the first reflection from the directly illuminated area.

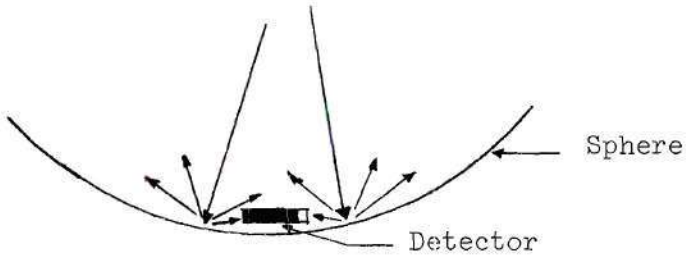

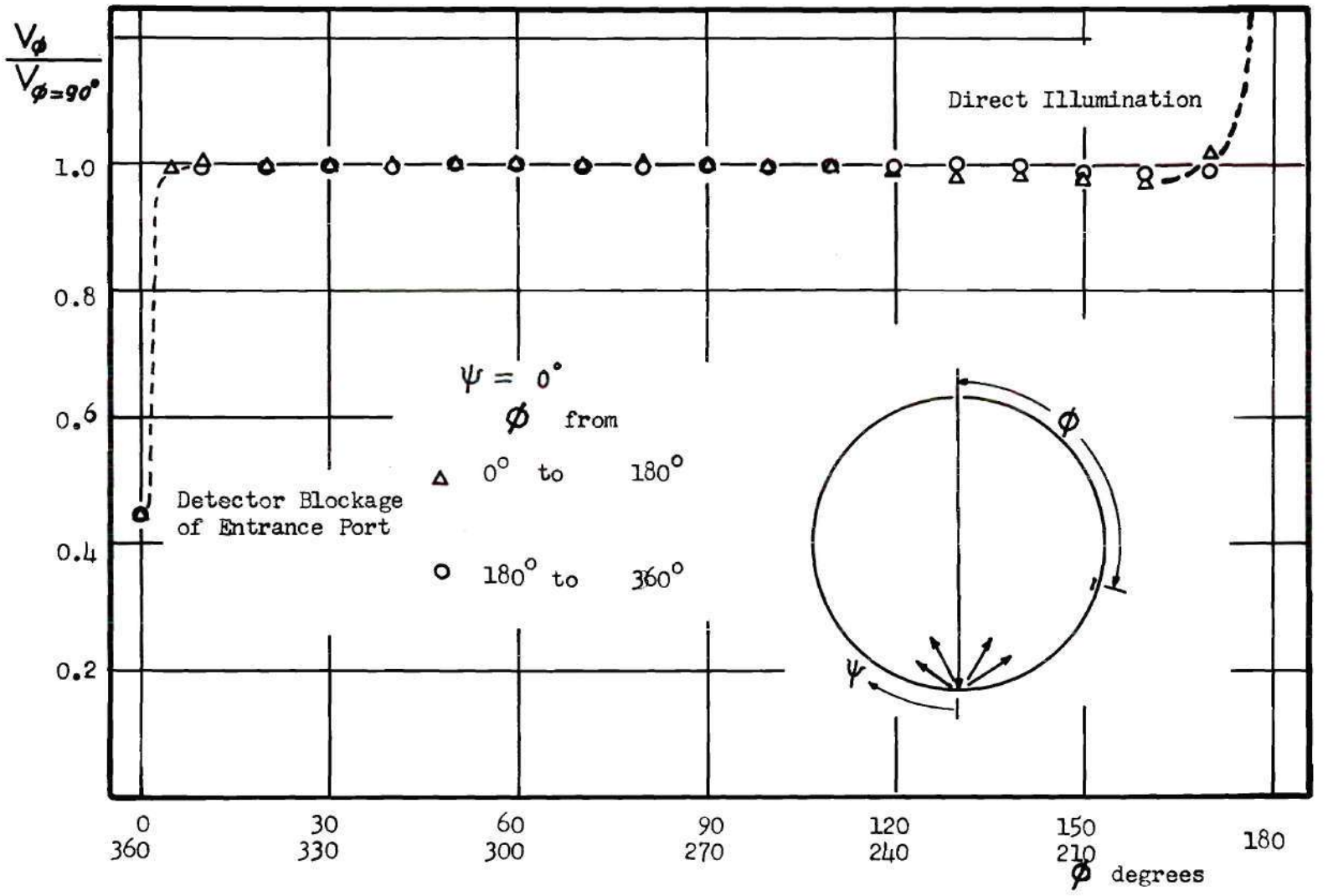

Figure 5. Irradiance on the Sphere Wall without Sample

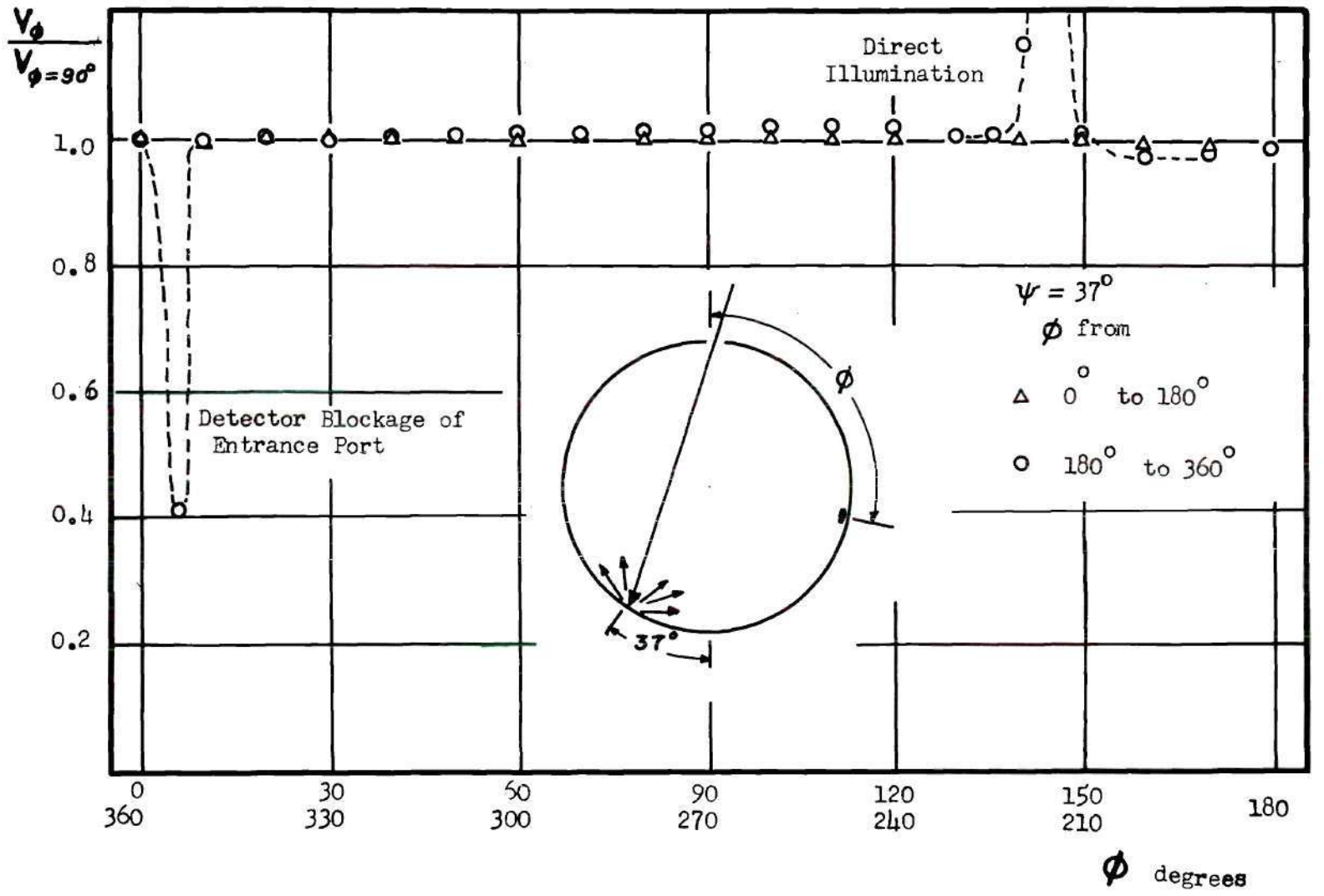

Figure 6. Irradiance on the Sphere Wall without Sample

Since only the black surface of the solar cell receives energy, the detected irradiance of the wall is not exactly symmetric about ϕ = 180 deg because of edge effect of the solar cell.

Irradiance on the Wall with Sample at the Center

The irradiance on the sphere wall for a center mounted sample will depend on whether the sample surface reflects diffusely or specularly. A perfectly diffuse reflecting surface was approximated by a MgO or carbon blackened surface at normal incidence and the other extreme, a specular reflector, by a polished aluminum surface.

Dawson, et al.[12], have shown that the irradiance on the wall depends not only on the reflection characteristics of the test sample but also on its size and the type of reflecting surface on the back side of the sample holder. Results of wall irradiance for various ratios of sphere to sample radius and upper to lower reflecting surfaces are shown in Figs. 7, 8, and 9.

Diffuse Reflecting Surfaces

Figure 7 shows the wall irradiance results for a $\frac{\text{MgO}}{\text{MgO}}$ surface system as a function of the ratio of sphere to sample radius. Two sets of data are shown, set A for the sample being illuminated for a zero angle of incidence, and set B for the wall being illuminated at Ψ = 37 deg. Data points are indicated for every 30 deg; however, the curves are fit through data points taken evey 10 deg.

The detected irradiance is normalized by the irradiance at ϕ = 90 deg without a sample inside the sphere. The reason that all irradiances are normalyzed by the irradiance at ϕ = 90 deg is that if the thickness

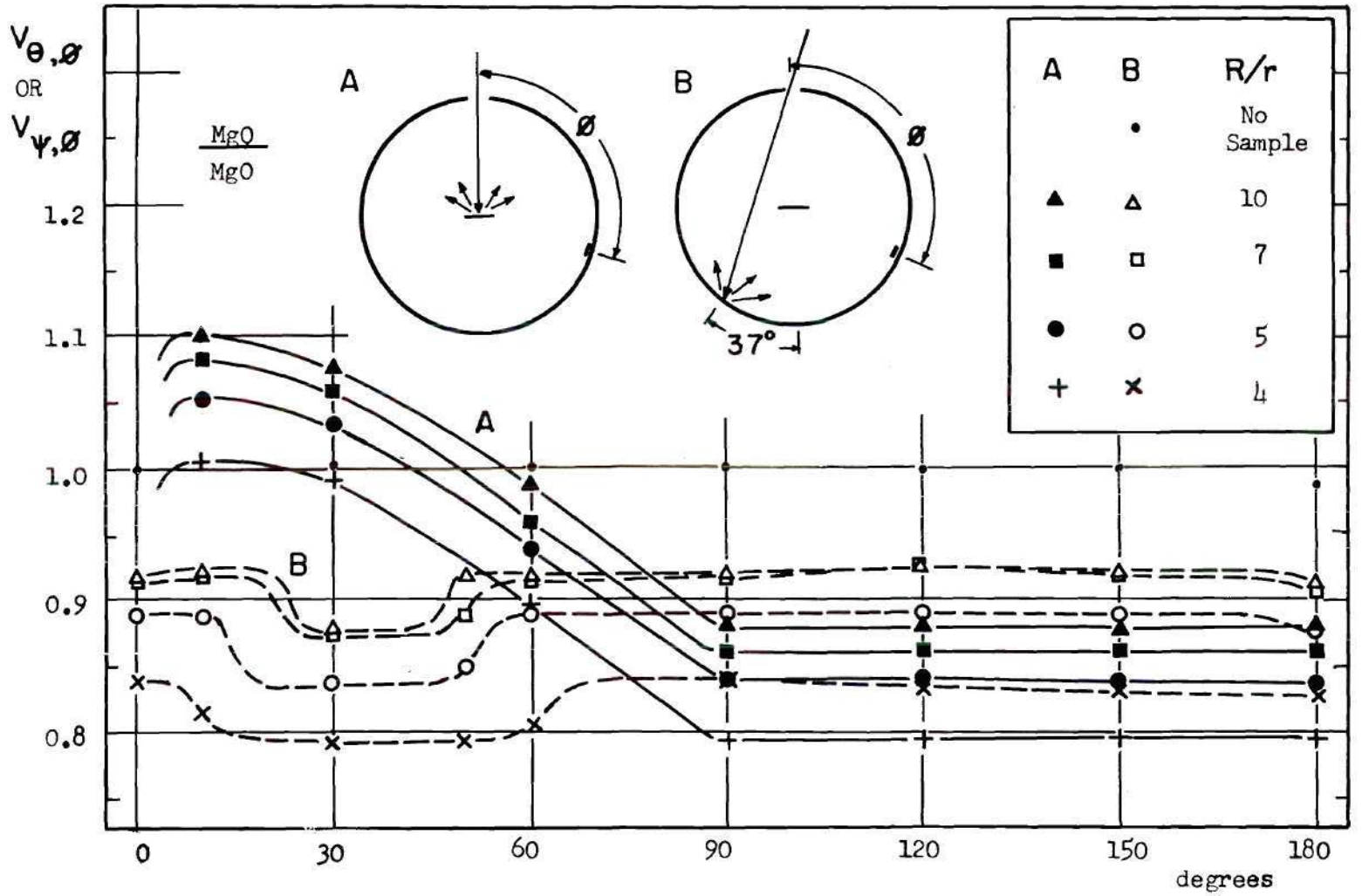

Figure 7. Irradiance on the Sphere Wall with $\frac{MgO}{MgO}$ System

of the test sample is neglected, then an infinitesimally small detector at ϕ = 90 deg can see every point of the inside sphere wall, and for a sample following Lambert's cosine law any energy reflected from the test sample surface cannot be detected. Also, almost all the previous investigators have placed the detector at ϕ = 90 deg. For a finite size detector centered at ϕ = 90 deg, however, the energy reflected from the sample will be detected.

If a perfectly diffuse reflecting sample is illuminated at the center of the sphere, the upper hemisphere receives more energy by virtue of the first reflection from the sample, while the lower hemisphere does not receive any energy from the first reflection as illustrated in Fig. 1. For such a system, the distribution of the irradiance in the upper hemisphere will follow nearly a cosine variation which is to be slightly modified by subsequent reflections from the wall. This behavior was first discussed by Dawson, et al.[12], and is verified by the data for set A in Fig. 7. The irradiance in the lower hemisphere is very uniform due to multiple reflections. The decrease of detected irradiance near ϕ = 180 deg when the sphere wall is illuminated at ϕ = 37 deg is caused by the inability of detector to receive the first reflection from the wall as discussed previously. Similar results were obtained for sample systems of $\frac{\text{MgO}}{\text{Black}}$, $\frac{\text{Black}}{\text{Black}}$, and $\frac{\text{Black}}{\text{MgO}}$ as shown in Fig. 8.

The lower irradiance for larger samples is caused by the sample blockage, since more energy hits the sample and is absorbed.

Specular Reflecting Surface

If the front surface of the test sample is specular reflecting, then only a small area on the upper hemisphere receives energy from the first

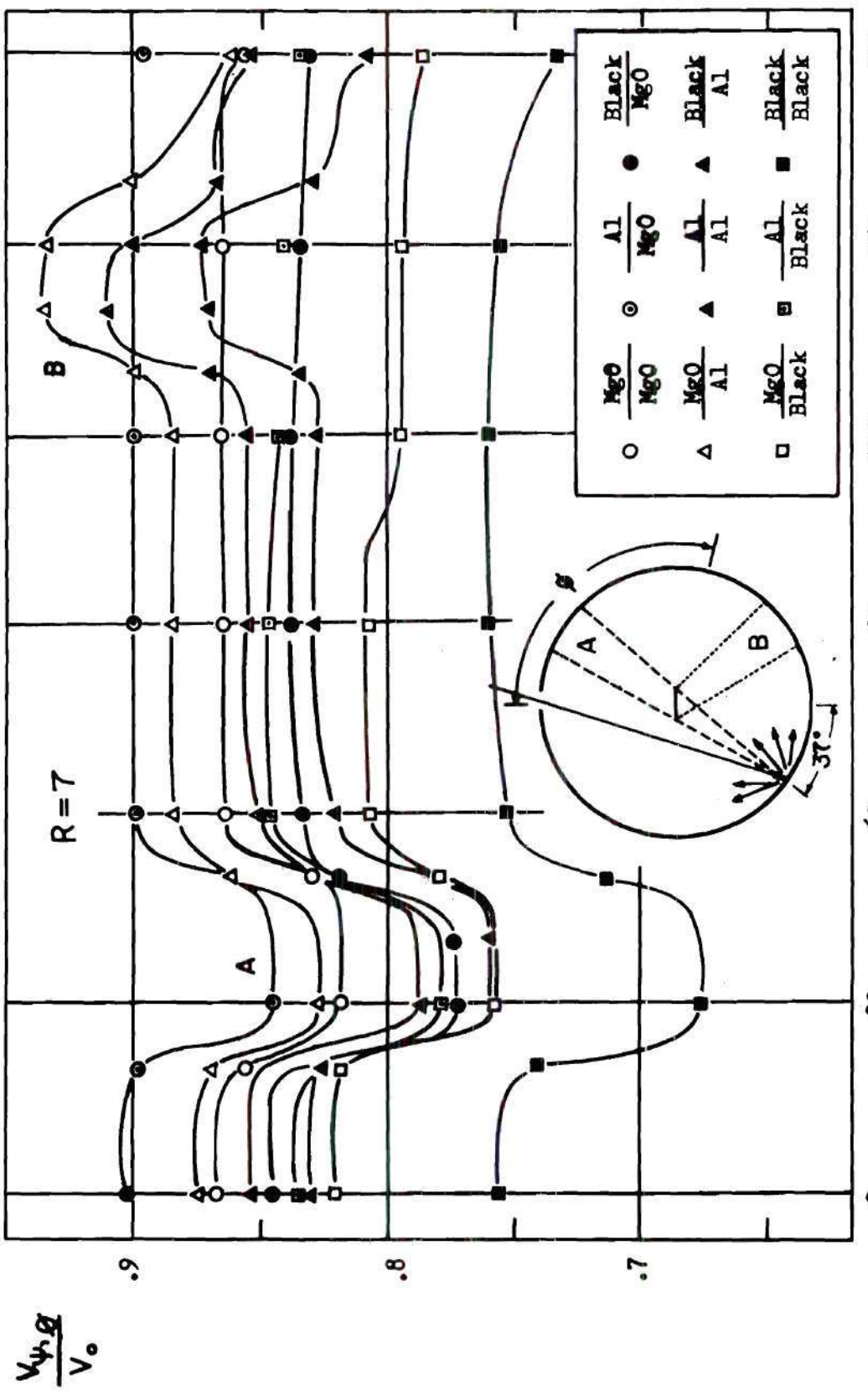

Figure 8. Irradiance on the Sphere Wall with Samples for Wall Illumination

reflection, and the irradiance on the wall is uniform except for this area and directly opposite area along the sphere diameter where the second reflection from the wall is blocked by the sample. Results of wall irradiance for a specular reflecting surface, $\frac{A1}{A1}$, for various angles of incidence are shown in Fig. 9. For $\theta = 0$ deg most of the incident energy is reflected back and out through the entrance port. The small irradiance for this case is due to the diffuse components of the aluminum surface. Even for $\theta = 5.6$ deg part of the incident energy leaves the sphere from the first reflection. The small variations may be caused by imperfect specular reflectance of the sample surface.

Effects of Centrally Located Sample on the Irradiance in the Upper Hemisphere

The following analysis is made assuming that a perfectly diffusely reflecting sample is at the center of the sphere and that after the first reflection from the sample, the sample blockage is negligible. Also, the effects of the finite size of the detector is neglected.

When the detector is in the upper hemisphere ($0^\circ \leq \phi \leq 90^\circ$), the detected irradiance from the first reflection from the sample surface, V_1^u, is proportional to cos ϕ.

$$V_1^u = \frac{4k\, A_d\, E_o\, \rho_{s_1}}{A} \cos \phi$$

The factor 4 comes from the fact that the radiation shape factor from the sample to the detector is $\frac{A_d}{\pi R^2} \cos \phi$, and the total area of the sphere $A = 4 \pi R^2$. The second reflection from the sphere wall will be diffused and neglecting the center mounted sample,

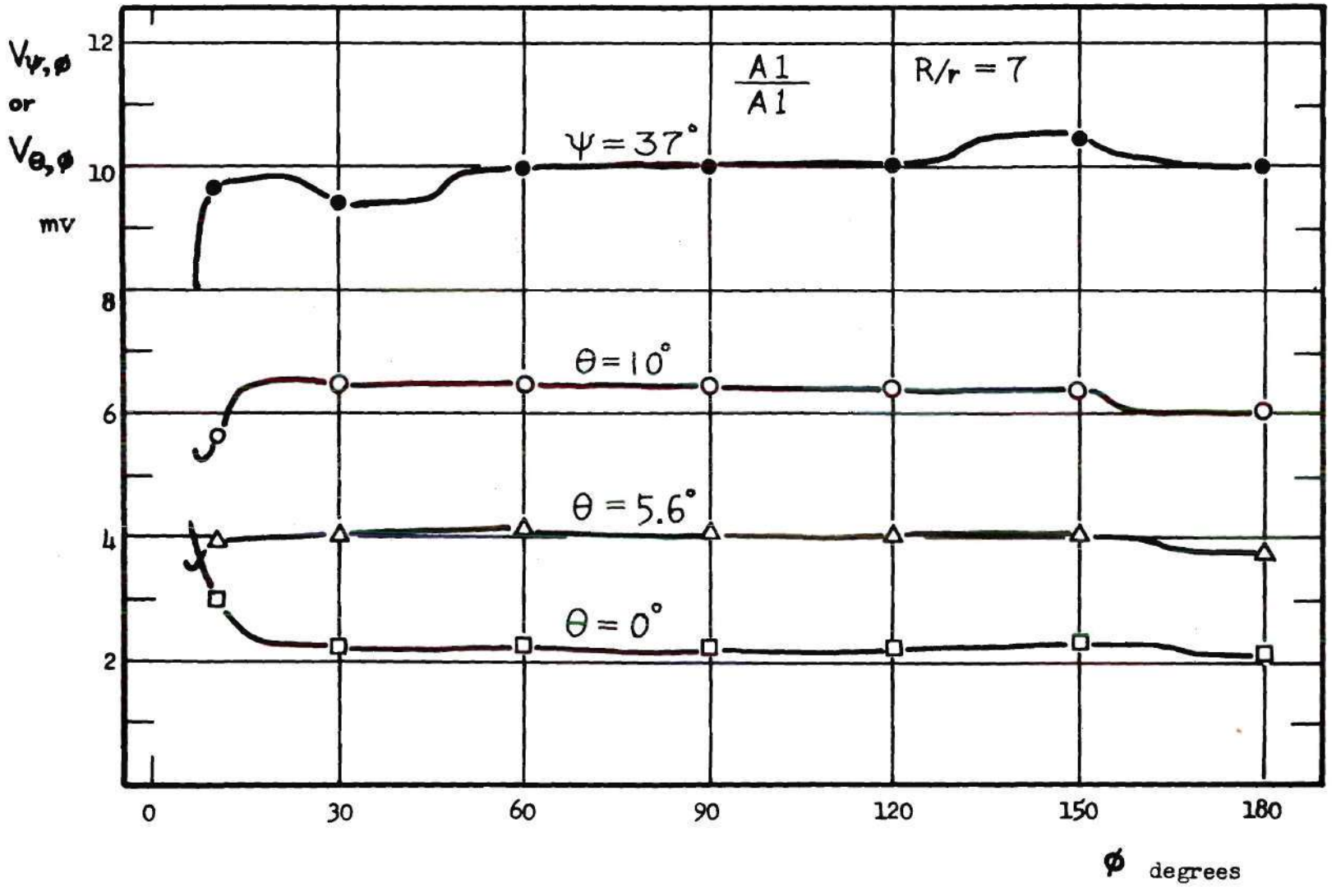

Figure 9. Irradiance on the Sphere Wall with Specularly Reflecting Samples

the detected irradiance from the second reflection, V_2^u, is

$$V_2^u = \int_0^{\pi/2} \frac{2k\, A_d\, E_o\, \rho_{s_1}\, \rho_w}{A} \sin \phi' \cos \phi' \, d\phi' \quad .$$

Carrying out the integration gives

$$V_2^u = \frac{k\, A_d\, E_o\, \rho_{s_1}\, \rho_w}{A} \quad .$$

Similarly, the detected irradiance from the third, fourth, ... reflections, V_3^u, V_4^u, ..., will be

$$V_3^u = \frac{k\, A_d\, E_o\, \rho_{s_1}\, \rho_w^{\,2}}{A}$$

$$V_4^u = \frac{k\, A_d\, E_o\, \rho_{s_1}\, \rho_w^{\,3}}{A}$$

$$\ldots \; .$$

The total detected irradiance, $V_{\theta,\phi}^u$, is then

$$V_{\theta,\phi}^u = \frac{k\, A_d\, E_o\, \rho_{s_1}}{A} (4 \cos \phi + \rho_w + \rho_w^{\,2} + \rho_w^{\,3} + \ldots)$$

$$V_{\theta,\phi}^u = \frac{k\, A_d\, E_o\, \rho_{s_1}}{A} \left(4 \cos \phi + \frac{\rho_w}{1 - \rho_w}\right) \qquad (1)$$

If the detector is in the lower hemisphere ($90^\circ \leq \phi \leq 180^\circ$), the first reflection from the sample is not detected, $V_1^1 = 0$. The detector

responses for the second, third, ... reflections from the sphere wall, V_2^1, V_3^1, ..., will be

$$V_2^1 = \frac{k\, A_d\, E_o\, \rho_{s_1}\, \rho_w}{A}$$

$$V_3^1 = \frac{k\, A_d\, E_o\, \rho_{s_1}\, \rho_w^2}{A}$$

... .

Summing over all reflections, the total detector response would be

$$V_{\theta,\phi}^1 = \frac{k\, A_d\, E_o\, \rho_{s_1}}{A} \frac{\rho_w}{1 - \rho_w} \quad . \tag{2}$$

For the case when detector is at $\phi = 90$ deg, both equations can be applied. Dividing Equation 1 by Equation 2, one obtains

$$\frac{V_{\theta,\phi}^u}{V_{\theta,\phi}^1} = 1 + \frac{4(1 - \rho_w)}{\rho_w} \cdot \cos \phi \quad . \tag{3}$$

Equation 3 is seen to be independent of the reflectance of the test sample. Figs. 10 and 11 show the experimental results for the ratio of the detector response in the upper hemisphere to that at the detector location of $\phi =$ 90 deg, $\frac{V_{\theta,\phi}^u}{V_{\phi = 90^o}}$. The solid lines in Figs. 10 and 11 are the calculated values from Equation 3 for a measured wall reflectance of $\rho_w = 0.965$ (see Appendix A).

The disagreement between measured and calculated results is caused by sample blockage effects, absorption of radiation by the front and back

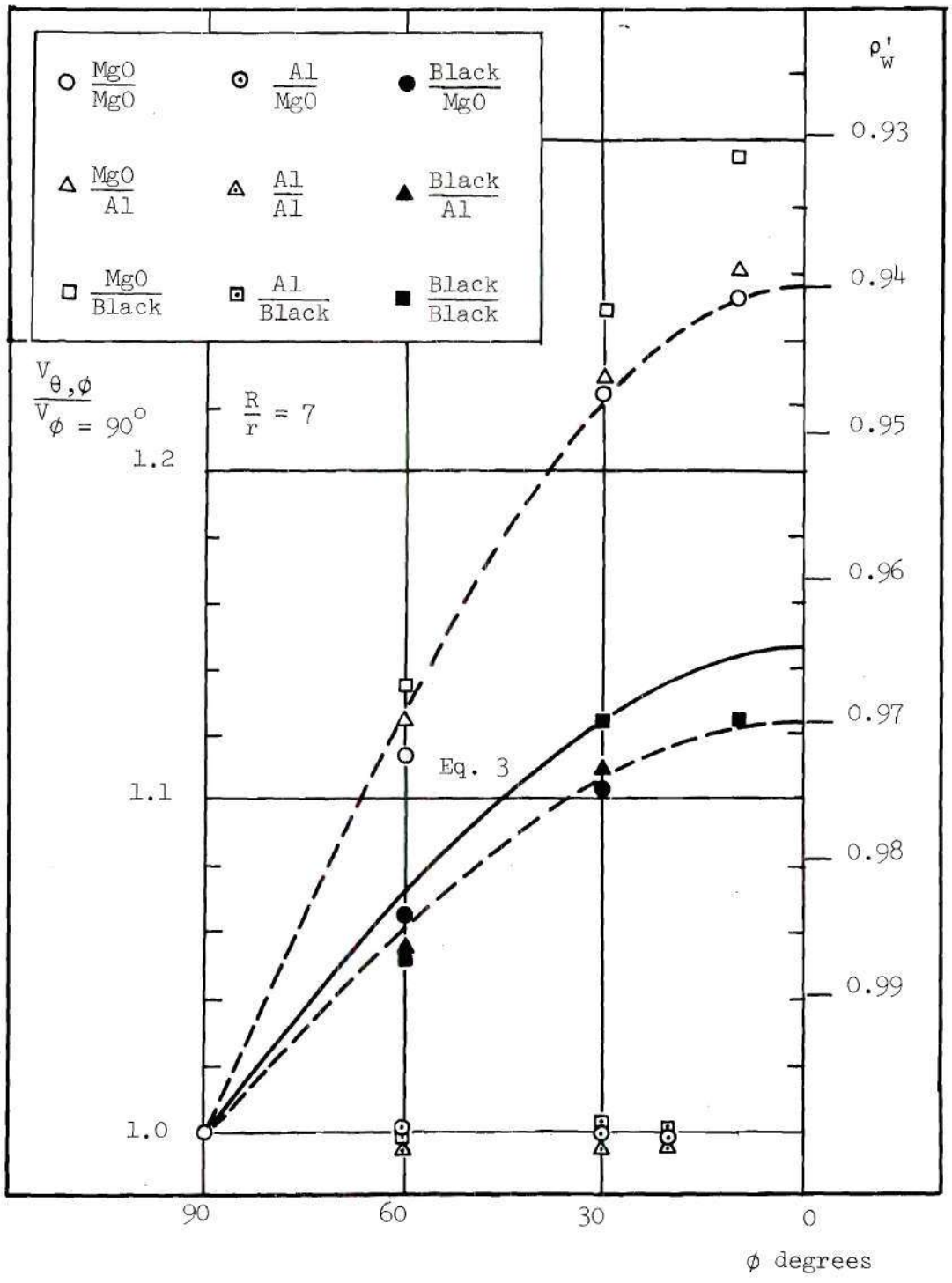

Figure 10. Irradiance Distribution in the Upper Hemisphere

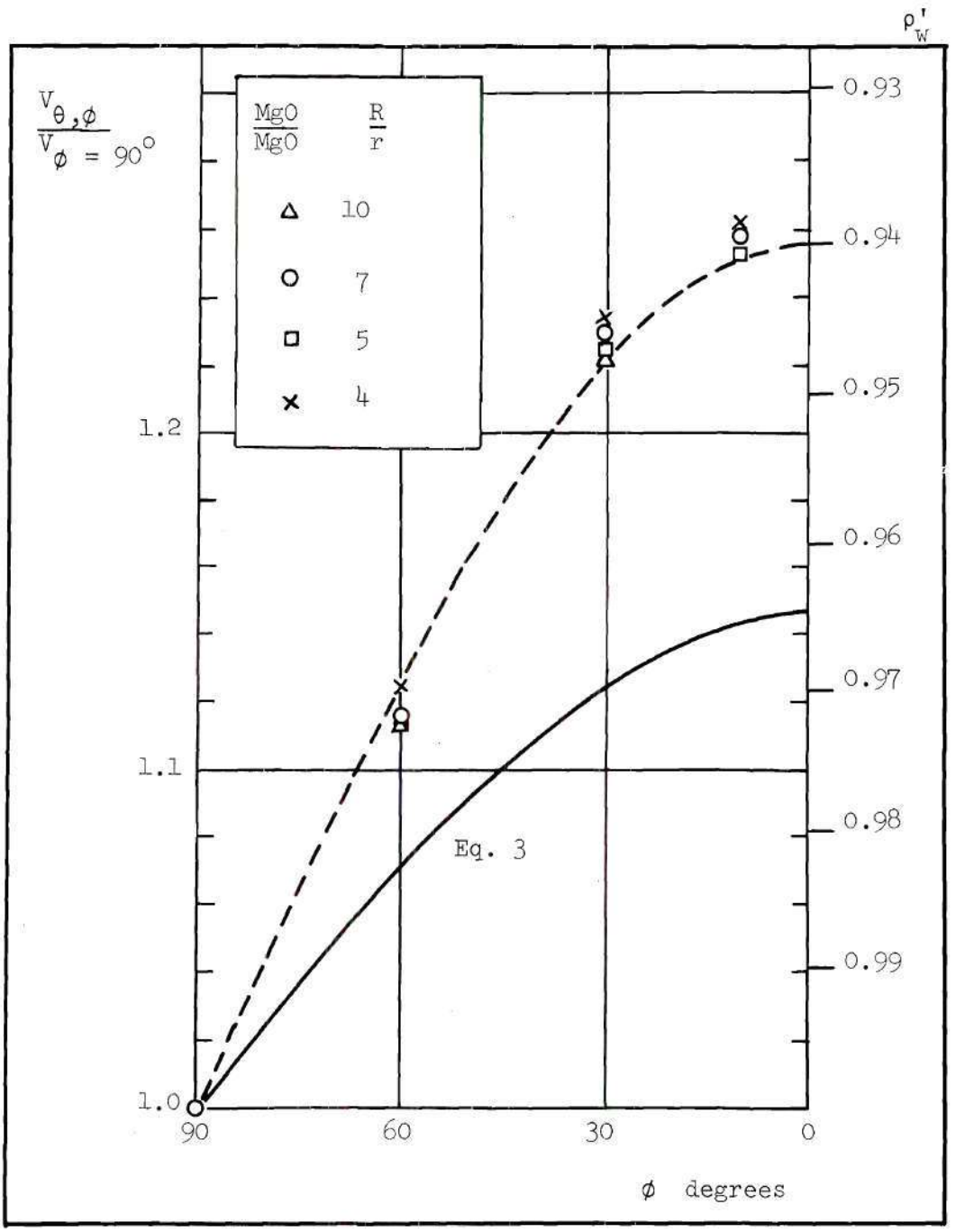

Figure 11. Irradiance Distribution in the Upper Hemisphere for $\frac{MgO}{MgO}$ System.

surfaces of the test sample, and because the test samples are not perfectly diffuse surfaces. That is, not only the first reflection but also the subsequent reflections affect the wall irradiance. For a diffuse sample every reflection from the surface is proportional to cos ϕ so that more energy will be reflected in the normal direction, thereby increasing the wall irradiance for small ϕ's. With this in mind, the effects of sample surface reflectances can be understood. The higher the reflectance of the upper surface of test sample, the higher will be the irradiance in the upper hemisphere. Also, the effect of the reflectance of the back side of the test sample can be reasoned to produce the opposite effect. This trend is evident in Fig. 10 where higher values of $\frac{V^u_{\theta,\phi}}{V_{\phi = 90^\circ}}$ are obtained for the sample system of $\frac{MgO}{Black}$ as compared to $\frac{MgO}{MgO}$. Equation 3 should be modified for this effect. However, the effect is small and will be neglected in further discussion. To predict the correct ratio $\frac{V^u_{\theta,\phi}}{V_{\phi = 90^\circ}}$, one needs to adjust the reflectance of the sphere wall, i.e., substitute an apparent reflectance of sphere wall surface, ρ_w', into Equation 3 instead of true reflectance, ρ_w. The dotted lines in Figs. 10 and 11 are calculated values of Equation 3 for apparent reflectances of $\rho_w' = 0.94$ and $\rho_w' = 0.97$. Also shown on the right side of Figs. 10 and 11 are the intercepts of Equation 3 for various values of ρ_w' as indicated.

The dependence of $\frac{V^u_{\theta,\phi}}{V_{\phi = 90^\circ}}$ on the sample size is shown in Fig. 11. The larger the sample, the more energy will be reflected to upper hemisphere. The dependence on the sample size is seen to be very small. This is because the area of illumination for the incident beam was the same for all samples and therefore the first reflection from the sample surface is independent of its size.

Sample Blockage Effects When the Wall is Illuminated

When the sphere wall is illuminated at $\Psi = 37$ deg with a test sample at the center, the first reflection from the wall is not seen by an area directly opposite on the sphere wall because of blockage by the sample. This is illustrated on the sphere diagram in Fig. 8. The size of this first-reflection-blocked area depends on the sample size as anticipated from geometric consideration. This effect is shown in Fig. 7 for the set B measurements.

If the detector is in this shaded area, and if one neglects the effect of the test sample at the center of the sphere after the first reflection from the wall, the detected irradiance, V_{sh}, will be, after similar calculations as in the last section,

$$V_{sh} = \frac{k A_d E_o}{A} \frac{\rho_w^2}{1 - \rho_w} \quad . \tag{4}$$

Now if the detector is not blocked by the test sample from the first reflection, the detected irradiance is

$$V_{\Psi,\phi} = \frac{k A_d E_o}{A} \frac{\rho_w}{1 - \rho_w} \quad . \tag{5}$$

Dividing Equation 4 by Equation 5, one obtains

$$\frac{V_{sh}}{V_{\Psi,\phi}} = \rho_w \quad . \tag{6}$$

For this case one can calculate the "approximate" reflectance of the sphere wall. Figure 12 shows the results calculated by Equation 6 of $\frac{V_{\phi = 37^o}}{V_{\phi = 90^o}}$ from

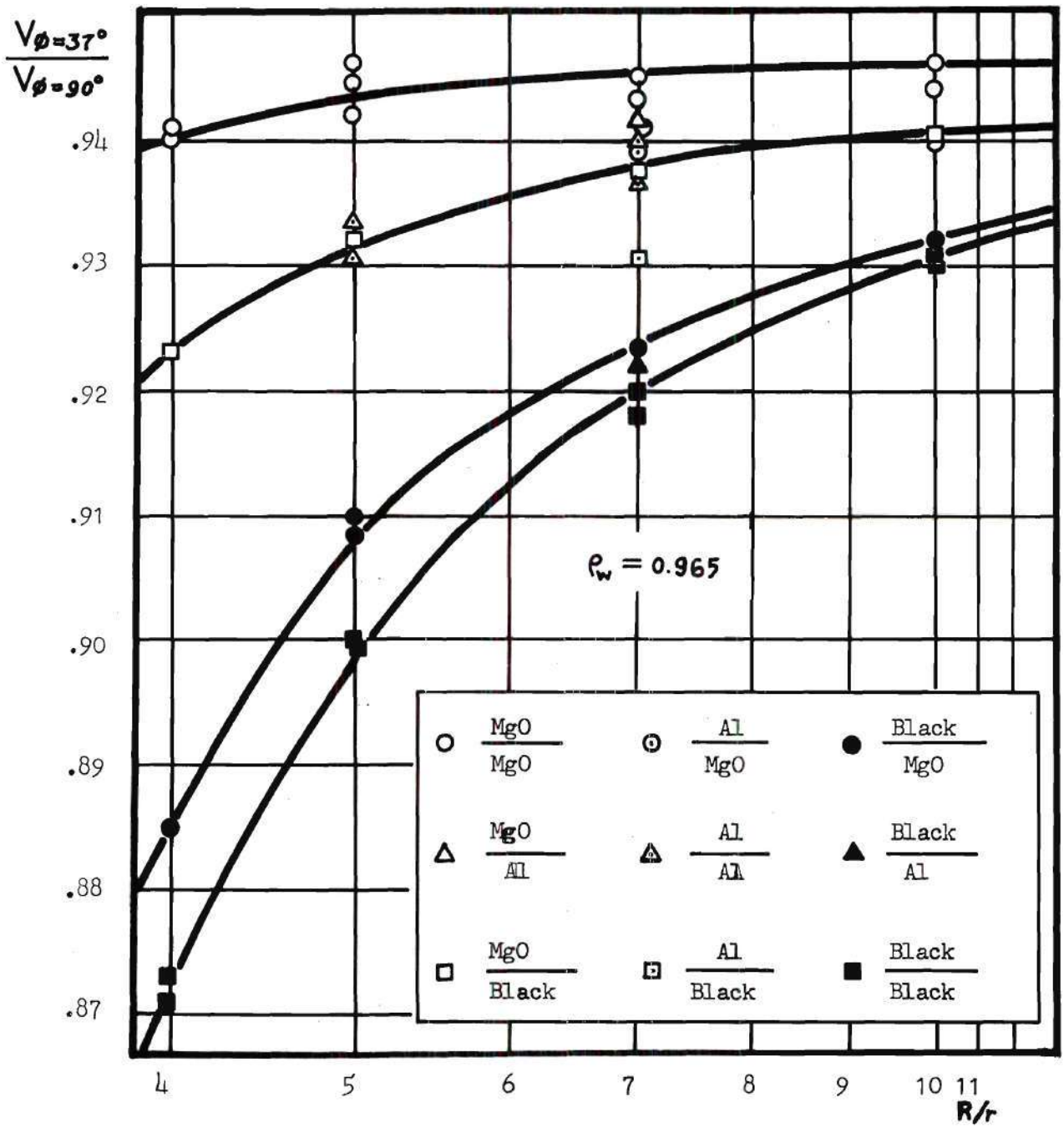

Figure 12. Sample Blockage Effects for Wall Illuminations

the experimental data. The disagreement of the results from the true reflectance of the wall surface is caused by the sample blockage and absorption effects. Also, the results show the possibility of measuring the reflectance of the sphere wall surface, if a small sample with ideally reflecting surfaces ($\rho_{s_1} = \rho_{s_2} = 1.0$) is used.

Another effect of interest is the increase of the detected irradiance near $\phi = 143$ deg when the back surface of the sample is specular reflecting (Fig. 8). This is easily explained by the specular reflection of the directly reflected energy from the wall at $\Psi = 37$ deg to the back side of the sample.

Reflectances of the Test Samples

Absolute Measurement Technique

Consider Equations 2 and 5 for the case that a diffuse sample or the sphere wall is illuminated and that the detector is in the lower hemisphere.

$$V^1_{\theta,\phi} = \frac{k A_d E_o \rho_{s_1}}{A} \frac{\rho_w}{1 - \rho_w} \tag{2}$$

$$V_{\Psi,\phi} = \frac{k A_d E_o}{A} \frac{\rho_w}{1 - \rho_w} \tag{5}$$

If Equation 2 is divided by Equation 5, one obtains

$$\frac{V^1_{\theta,\phi}}{V_{\Psi,\phi}} = \rho_{s_1} . \tag{7}$$

However, if the detector is in the upper hemisphere, then Equation 3 must be used instead of Equation 2.

$$V^{u}_{\theta,\phi} = \frac{k A_d E_o \rho_{s_1}}{A} \left(4 \cos \phi + \frac{\rho_w}{1 - \rho_w}\right) \tag{3}$$

If Equation 3 is divided by Equation 5, one obtains

$$\frac{V^{u}_{\theta,\phi}}{V_{\Psi,\phi}} = \rho_{s_1} \left\{ 1 + \frac{4(1 - \rho_w)}{\rho_w} \cos \phi \right\} ,$$

or

$$\rho_{s_1} = \frac{V^{u}_{\theta,\phi}}{V_{\Psi,\phi} \left\{ 1 + \frac{4(1 - \rho_w)}{\rho_w} \cos \phi \right\}} . \tag{8}$$

For the specular reflecting samples, Equation 7 is applied for both cases, the upper and lower hemispheres. Equation 7 has been used by many investigators[9,10,13], without taking into account of the effects of a centrally located sample. In this study only Equation 7 is used for the calculations of reflectances of the samples.

The results of $\frac{V^{l}_{\theta,\phi}}{V_{\Psi,\phi}}$ are shown in Figs. 13, 14, and 15. The dashed lines are separately measured reflectances of the upper surfaces of the test samples (see Appendix A). The variations of this ratio with angle are due mostly to the variations of detected irradiance, $V_{\Psi,\phi}$, when the wall is illuminated, since the detected irradiance in the lower hemisphere, $V^{l}_{\theta,\phi}$, is almost uniform when the sample is illuminated (Figs. 7 and 8).

Figure 13 shows that samples with MgO coated back surfaces have

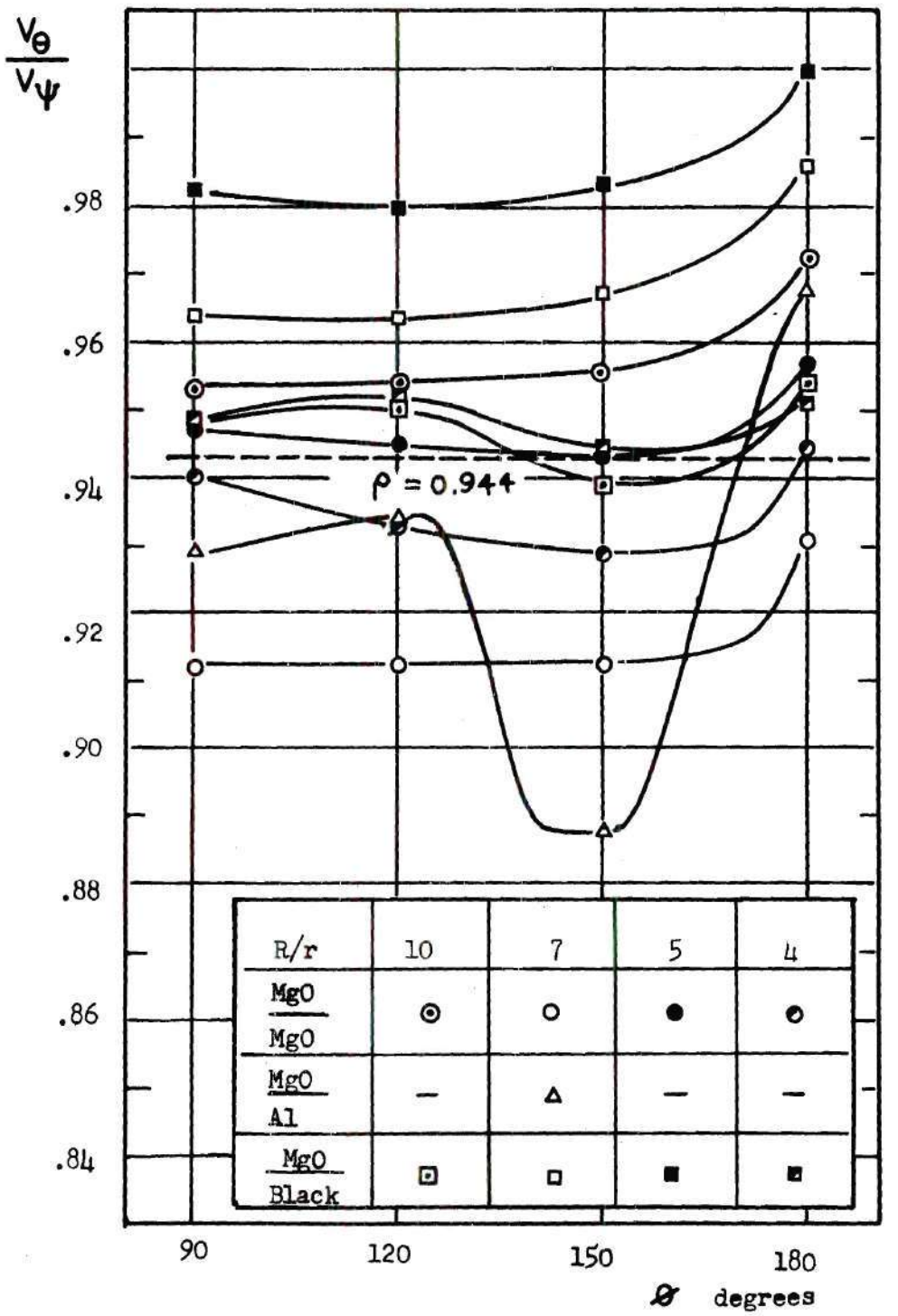

Figure 13. Reflectance of MgO Coated Surfaces Measured by Absolute Technique

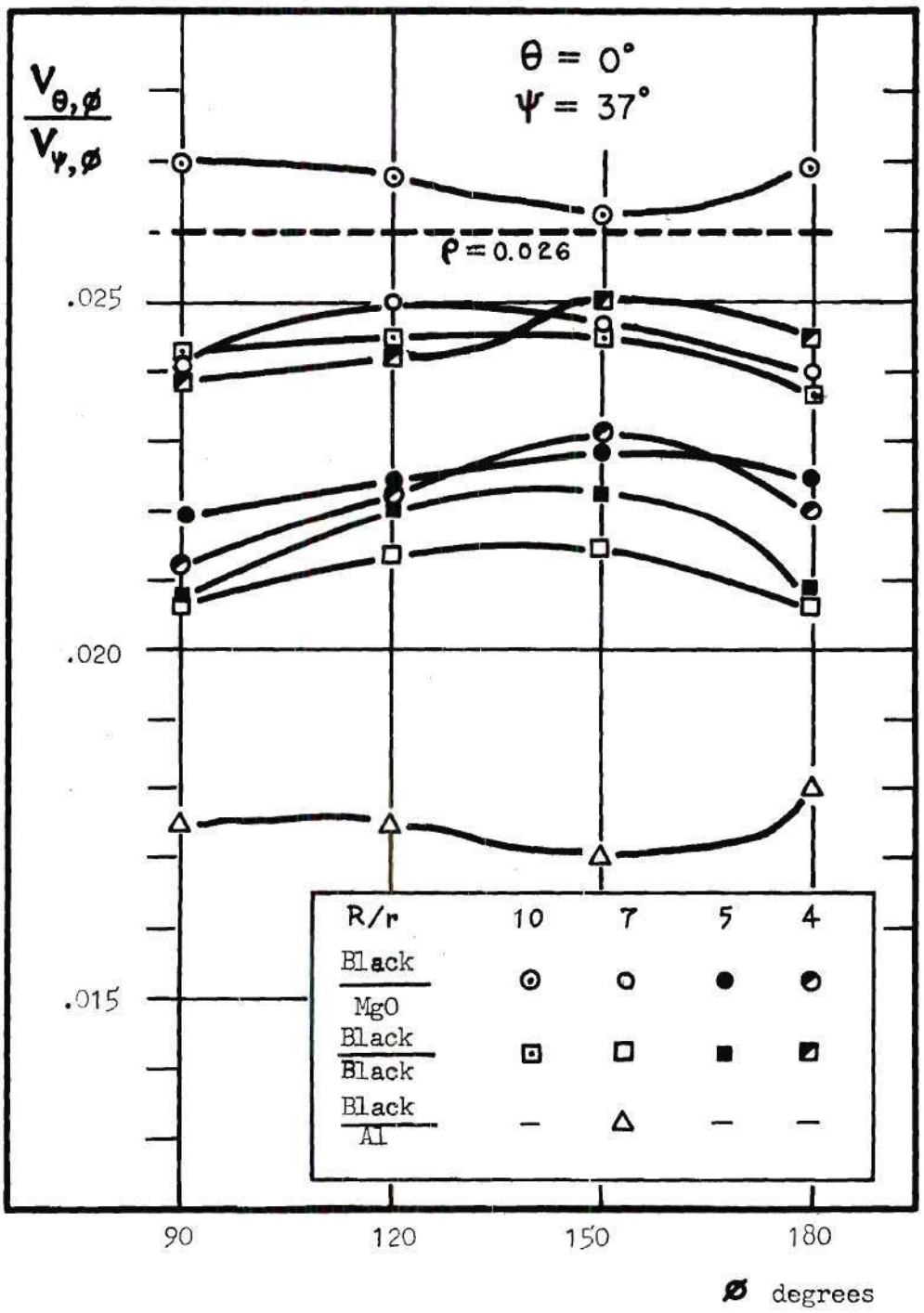

Figure 14. Reflectance of Carbon Blackened Surfaces Measured by Absolute Technique

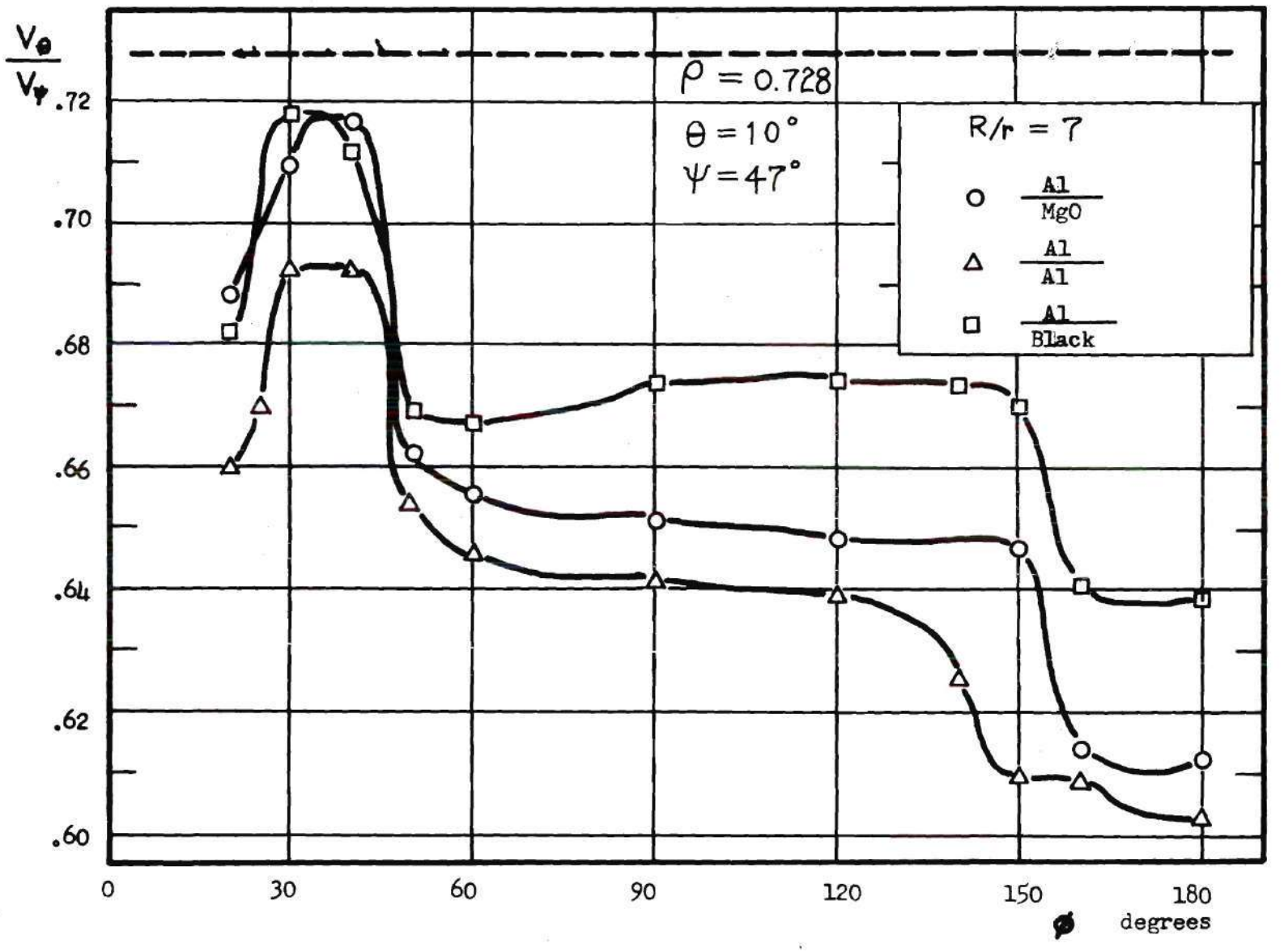

Figure 15. Reflectance of Polished Aluminum Surfaces Measured by Absolute Technique

apparently smaller values of $\frac{V^1_{\theta,\phi}}{V_{\Psi,\phi}}$. The reason for this is that less energy is absorbed by the back surface and therefore more energy is available for wall illumination. That is, $V_{\Psi,\phi}$ is the larger for $\frac{MgO}{MgO}$ than $\frac{MgO}{Black}$ systems. It also shows smaller errors for the large samples (R/r = 4), but this is thought to be caused by compensating errors in the detected irradiance measurements. Similar results were also obtained by Dawson, et al.[12]. The sudden decrease of $\frac{V^1_{\theta,\phi}}{V_{\Psi,\phi}}$ near ϕ = 180 deg is caused by experimental errors due to the detector displacement from the wall.

Figure 14 shows similar trend for the carbon blackened test samples. Both Fig. 13 and Fig. 14 show higher $\frac{V^1_{\theta,\phi}}{V_{\Psi,\phi}}$ for smaller ρ_{s_2}, which can be explained from the distribution of irradiance on the wall with a sample at the center as discussed in the previous section.

Figure 15 shows the ratio $\frac{V_{\theta,\phi}}{V_{\Psi,\phi}}$ for samples with specularly reflecting upper surfaces. The errors are relatively large, even though the angle of incidence, θ, is 10 deg so that the first reflection from the sample will not hit the entrance port. The reason for this is thought to be caused by the energy that leaves the sphere through the entrance port. The increase of the ratios near ϕ = 37 deg is caused by the decrease of $V_{\Psi,\phi}$, while the decrease of the ratios, $\frac{V_{\theta,\phi}}{V_{\Psi,\phi}}$, hear ϕ = 180 deg is caused by the decrease of $V_{\theta,\phi}$.

Relative Measurement Technique

For the cases when the center mounted sample is illuminated, Equations 1 and 2 apply for the upper and lower hemispheres, respectively.

$$V^u_{\theta,\phi} = \frac{k\, A_d\, E_o\, \rho_{s_1}}{A} \left(4 \cos \phi + \frac{\rho_w}{1 - \rho_w}\right) \qquad (1)$$

$$V^{l}_{\theta,\phi} = \frac{k\, A_d\, E_o\, \rho_{s_l}}{A} \frac{\rho_w}{1 - \rho_w} \quad . \tag{2}$$

Substituting apparent sphere wall reflectance, ρ_w', as discussed before, one obtains

$$V^{u}_{\theta,\phi} = \frac{k\, A_d\, E_o\, \rho_{s_l}}{A} \left(4 \cos \phi + \frac{\rho_w'}{1 - \rho_w'}\right) \tag{9}$$

$$V^{l}_{\theta,\phi} = \frac{k\, A_d\, E_o\, \rho_{s_l}}{A} \frac{\rho_w'}{1 - \rho_w'} \quad . \tag{10}$$

If a diffuse reference surface whose reflectance is known replaces the test sample at the center of the sphere and is illuminated, one obtains

$$V^{u}_{r} = \frac{k\, A_d\, E_o\, \rho_r}{A} \left(4 \cos \phi + \frac{\rho_w'}{1 - \rho_w'}\right) \tag{11}$$

$$V^{l}_{r} = \frac{k\, A_d\, E_o\, \rho_r}{A} \frac{\rho_w'}{1 - \rho_w'} \quad . \tag{12}$$

If the detector is at the same position for both cases, and Equation 9 divided by Equation 11, or Equation 10 divided by Equation 12, one obtains

$$\frac{V^{u}_{\theta,\phi}}{V^{u}_{r}} = \frac{V^{l}_{\theta,\phi}}{V^{l}_{r}} = \frac{\rho_{s_l}}{\rho_r} \quad , \tag{13}$$

or

$$\rho_{s_l} = \rho_r \frac{V_s}{V_r} \quad . \tag{14}$$

Equation 14 has been used by many investigators[7-10]. They, however, did not discuss the effects of the reflectance of back surfaces, since Equation 14 is independent of ρ_{s_2}. Equation 14 also shows no dependence on the detector location. However, as discussed in the previous sections, the irradiance on the sphere wall depends on the reflectance of back surface and on the detector location, and these factors would cause an error in the measurements of reflectance, even though the exact value of the reflectance of the reference surface is used.

Edwards, et al.[9], have put the reference surface on the back of the sample holder. This procedure may result in large errors in the reflectance measurements. For example, consider the case of a test sample with low reflectance and highly reflecting reference surface. Then more energy will be absorbed by the back surface when the reference surface is illuminated than when the test sample surface is illuminated.

Also, an error will be introduced if both test and reference surfaces do not have the same type of reflection characteristics. To show this, consider the case that the reference surface is perfectly diffuse following Lambert's cosine law but that the test sample has a high directional reflectance for large angle of reflection, for instance, see the results of Torrance, et al.[14]. If the detector is centered about $\phi = 90$ deg, it receives a larger portion of reflected energy from the test sample than from the reference surface and the result would give higher apparent reflectance of the test sample.

For perfectly specularly reflecting surfaces, Equation 10 applies both in the upper and lower hemispheres. If the reference surface is still diffusely reflecting, Equations 10 and 11 must be used for the case

that the detector is in the upper hemisphere. If Equation 10 is divided by Equation 11, one obtains

$$\frac{V_{\theta,\phi}}{V_r} = \frac{\rho_{s_1}}{\rho_r} \left(\frac{\frac{\rho_w'}{1 - \rho_w'}}{4 \cos \phi + \frac{\rho_w'}{1 - \rho_w'}} \right) , \qquad (15)$$

or

$$\rho_{s_1} = \rho_r \frac{V_s}{V_r} \left\{ 1 + \frac{4 (1 - \rho_w')}{\rho_w'} \cos \phi \right\} . \qquad (16)$$

For the case that the detector is in the lower hemisphere, Equation 14 applies also for the specularly reflecting samples.

Figures 10 and 17 are the reflectances of carbon blackened and polished aluminum surfaces measured relative to MgO coated surface. The reflectance of the reference surface $\rho_r = 0.944$ was used for MgO surface (Appendix A). The dependence of the measured reflectance values on the reflectance of the back surfaces are evident from Fig. 16. The calculated reflectances of carbon blackened surfaces are uniform in the lower hemisphere while they decrease in the upper hemisphere. This is because the apparent reflectance of the sphere wall used in Equations 9 - 12, ρ_w', depends on the reflectances of the front and back surfaces of the test sample (Fig. 10). For the specularly reflecting surfaces the angle of incidence was 10 deg, while that for the reference surface was zero deg (Fig. 17). The reflectance values are calculated only for the lower hemisphere for specularly reflecting samples. It is hard to give numerical discussions because

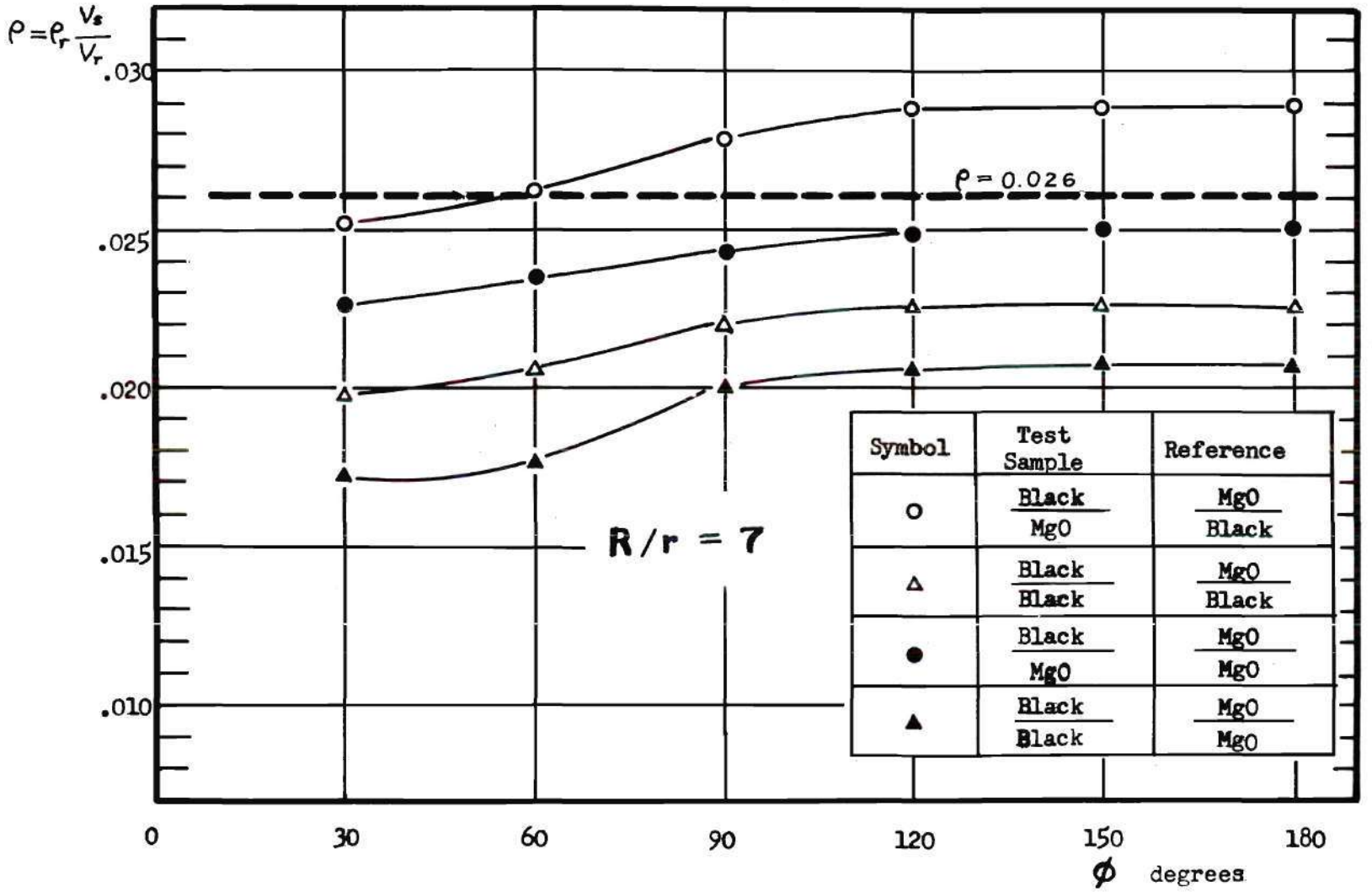

Figure 16. Reflectance of Carbon Blackened Surfaces Measured by Relative Technique

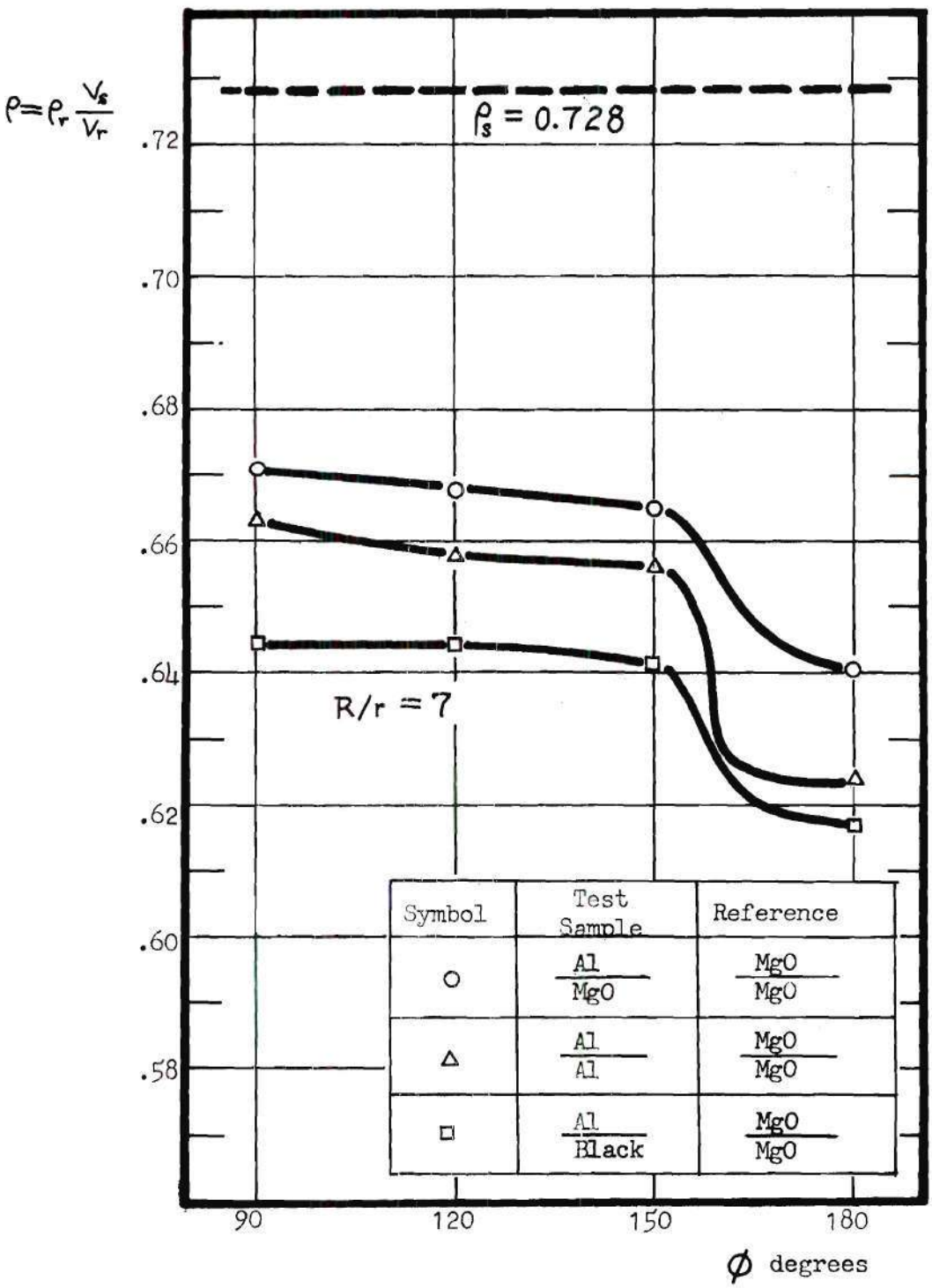

Figure 17. Reflectance of Polished Aluminum Surfaces Measured by Relative Technique

the experimental errors are relatively large.

CHAPTER V

CONCLUSIONS

In the modified integrating sphere, the irradiance distribution on the sphere wall is affected by the center mounted test sample. When a diffusely reflecting surface at the center is illuminated, the irradiance in the upper hemisphere has nearly a cosine distribution, while the irradiance in the lower hemisphere is almost uniform.

If the test sample surface is specularly reflecting, the irradiance on the sphere wall is uniform except for small areas caused by the first specular reflection from the test sample.

It has been shown that the irradiance on the sphere wall depends on sample size, reflectances of both upper and lower surfaces of test sample, and detector location.

For absolute measurement of angular-hemispherical reflectances, errors are introduced by the blockage effects of the center mounted test samples and the absorption effects by the front and back surfaces of the test samples. Errors will be introduced even in relative measurements if one uses different back surfaces for the test sample and reference surfaces. Also, it is shown that the calculated values of reflectances by relative technique decrease if the detector is in the upper hemisphere.

CHAPTER VI

RECOMMENDATIONS

The following studies are suggested for improving the uses of the modified integrating sphere.

(1) Analytic and experimental studies of the errors as a function of reflectances of the test sample and angle of incidence in relative measurement techniques.

(2) The effects of illumination area on the test sample.

(3) Errors of reflectances for non-perfectly diffuse samples.

APPENDIX A

MEASUREMENT OF "ABSOLUTE" REFLECTANCE

Diffuse Surfaces

The "absolute" reflectances of sample surfaces are measured by the classical method. The simplified diagram of the integrating sphere for this measurement is shown in Fig. 18. The test sample of 0.7 inches in diameter is illuminated with a shield between the sample and the detector so that the detector cannot receive the first reflection from the sample. The detector response in this case, V_s, is, if one assumes uniform irradiance on the sphere wall,

$$V_s = \frac{k A_d E_o \rho_s}{A} \frac{\rho_w}{1 - \rho_w} \quad . \tag{17}$$

Adjusting the collimating tube angle, the sphere wall is now illuminated, where the first reflection from the wall can be detected. Then the detector response, V_w, is

$$V_w = \frac{k A_d E_o \rho_w}{A} \frac{1}{1 - \rho_w} \quad . \tag{18}$$

If Equation 17 is divided by Equation 18, one obtains

$$\rho_s = \frac{V_s}{V_r} \quad . \tag{19}$$

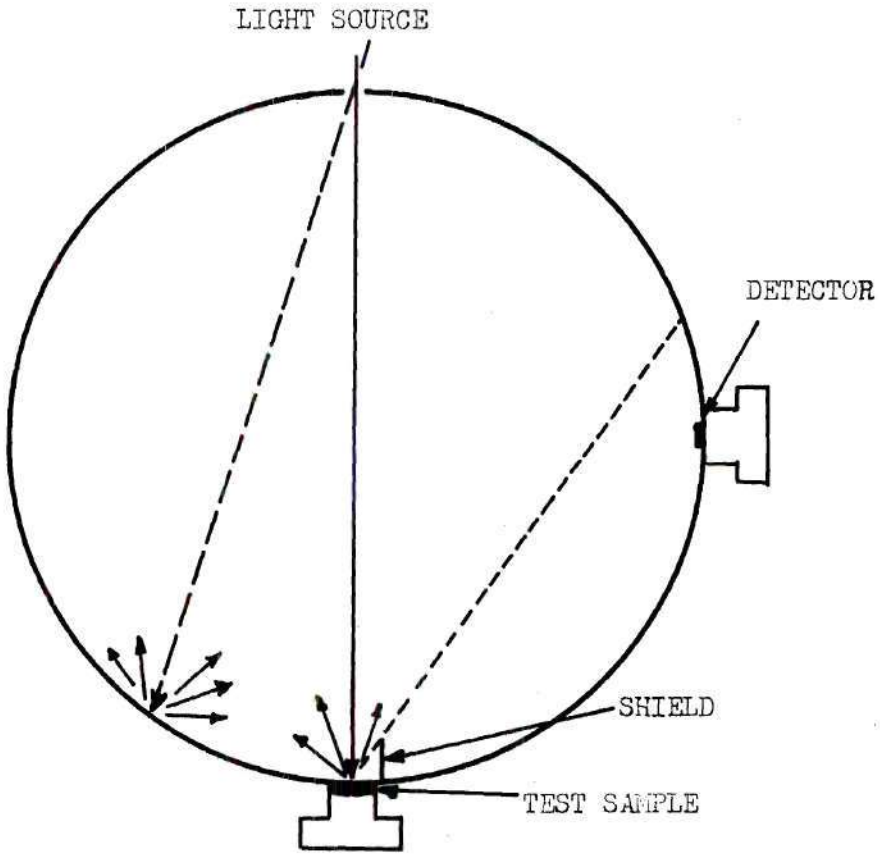

Figure 18. Integrating Sphere for "Absolute" Measurement of Reflectance

The same procedure is repeated and the results are averaged to obtain "absolute" reflectance of the surface.

Specularly Reflecting Surfaces

For a polished aluminum surface the same procedure is applied except an additional precaution is used to tilt the sample so that the first reflection from it will not hit the entrance port. The same equation applies in this case as for the diffuse surfaces.

Reflectance of Sphere Wall

After the measurement of the irradiance, V_s, as in the previous section, the sample holder is now turned so that the sample is seen by the detector, and is illuminated. The detector response, V_s', is

$$V_s' = \frac{k A_d E_o \rho_s}{A} \frac{1}{1 - \rho_w} \tag{20}$$

Dividing Equation 15 by Equation 18, one obtains

$$\rho_w = \frac{V_s}{V_s'}, \tag{21}$$

Results

Uniform irradiance distribution on the sphere wall was assumed to derive Equations 17, 18, and 20. But as discussed in Chapter IV, the shield causes some nonuniformities in the wall irradiance and a small error in the measurements will result. The measured results calculated by Equations 19 and 21 are shown in Table 1.

The different reflectances of MgO coated surfaces, the test sample

and sphere wall, are expected because of different thicknesses of MgO coatings. The results are seen to agree with previous measurements (15, 16, 17, and 18).

Table 1. Reflectances of Sample Surfaces and Wall Surface

SURFACES	MgO COATING			CARBON BLACK (Eq. 19)	POLISHED ALUMINUM (Eq. 19)
	SAMPLE (Eq. 19)	SPHERE WALL (Eq. 21)			
		with MgO	with CARBON BLACK		
NUMBERS OF MEASUREMENT	65	24	18	33	36
MEDIUM	.944	.965	.968	.0260	.728
MODE	.941	.874	.969	.0260	.729
MIDRANGE	.944	.959	.970	.0257	.728
RANGE	.018	.069	.044	.0019	.013
MEAN	.943	.963	.968	.0260	.729
STANDARD DEVIATION	.00356	.0154	.0118	.00049	.01155
"ABSOLUTE" REFLECTANCE	.944	.965		.0260	.728

APPENDIX B

EXPERIMENTAL ERRORS

Besides the analytical errors discussed in the main chapters, there are errors caused also by experimental procedures. Main sources of experimental errors are:

(1) Nonlinear response of detector and/or recorder,

(2) Incorrect reference values for relative measurements,

(3) Variation of light sources,

(4) Transient effects such as heating of the sphere wall, sample, and/or detector,

(5) Measurements of angles,

(6) Random errors such as reading values, variations in sample conditions, etc.

Also in this study the errors caused by the detector displacement from the sphere wall are very large in certain areas of the sphere wall as discussed in Chapter IV.

The errors due to nonlinear response of detector and/or recorder can be avoided if one corrects the results according to the characteristics of detector response.

The reference values, such as the reflectances of reference surface and sphere wall, cause errors if incorrect values are used. The transient effects can be avoided by waiting a long time to obtain steady state conditions for each reading, but this may cause another error if the

detector and/or sample surface have strong dependence of their characteristics on temperature, since each reading will have a different steady state temperature.

Each set of experimental conditions was repeated at least ten times to minimize random errors.

The maximum errors in this study can be evaluated from Equations 2, 7, and 14. Taking logarithm of Equation 2, one obtains

$$\text{Ln } V^{1}_{\theta,\phi} = \text{Ln } \left(\frac{k A_d E_o \rho_{s_1}}{A} \frac{\rho_w}{1 - \rho_w}\right) \quad . \tag{22}$$

Now if Equation 22 is differentiated, one obtains

$$\frac{\Delta V^{1}}{V^{1}} = \frac{\Delta k}{k} + \frac{\Delta E_o}{E_o} + \frac{\Delta \rho_{s_1}}{\rho_{s_1}} + \frac{\Delta \rho_w}{\rho_w} - \frac{\Delta(1 - \rho_w)}{1 - \rho_w} \quad , \tag{23}$$

So the maximum error in the irradiance distribution is

Detector response	$\frac{\Delta k}{k}$	= 1.0 per cent
Light source	$\frac{\Delta E_o}{E_o}$	= 0.5 per cent
Reflectance of sphere wall	$\frac{\Delta \rho_w}{\rho_w}$	= 1.0 per cent
Reflectance of sample	$\frac{\Delta \rho_{s_1}}{\rho_{s_1}}$	= 1.0 per cent
Random errors		0.5 per cent
Maximum possible error		4.0 per cent

The maximum possible error in the reflectance measured by absolute technique from Equation 7 is 2 x 4.0 = 8.0 per cent. Also the maximum error in the measurements of reflectance by relative technique from Equation 22 is 2 x 4.0 + 1.0 = 9.0 per cent.

LITERATURE CITED

1. R. V. Dunkle, "Spectral Reflectance Measurements," Surface Effects on Spacecraft Material, F. J. Clauss (ed.), John Wiley and Sons, Inc., 1960, p. 117.

2. A. H. Taylor, "A Simple Portable Instrument for the Absolute Measurement of Reflection and Transmission Factors," Scientific Papers, U. S. National Bureau of Standards, Vol. 17, No. 405, 1934, p. 165.

3. J. A. Jacquez and H. F. Kuppenheim, "Theory of the Integrating Sphere," Journal of the Optical Society of America, Vol. 45, 1955, p. 460.

4. J. A. Jacquez, W. McKeehan, J. Huss, J. M. Dimitroff, and H. F. Kuppenheim, "Integrating Sphere for the Measurement of Reflectance with the Beckman Model DR Recording Spectrophotometer," Journal of the Optical Society of America, Vol. 45, 1955, p. 971.

5. B. J. Hisdal, "Reflectance of Nonperfect Surfaces in the Integrating Sphere," Journal of the Optical Society of America, Vol. 55, 1965, p. 1255.

6. R. V. Dunkle, D. K. Edwards, J. T. Gier, and J. T. Bevans, "Solar Reflectance Integrating Sphere," Solar Energy, Vol. 4, 1960, p. 27.

7. B. E. Wood, B. A. McCullough, and J. P. Dawson, "Vacuum Integrating Spheres for Measuring Cryodeposit Reflectances from 0.35 to 15 Microns," AEDC-TR-65-1786 (AD 46808), 1965.

8. R. C. Eberhart, "Angular Dependence of Spectral Reflectance in the Infrared," M. S. Thesis, University of California, 1960.

9. D. K. Edwards, J. T. Gier, K. E. Nelson, and R. D. Roddick, "Integrating Sphere for Imperfectly Diffuse Samples," Applied Optics, Vol. 51, 1961, p. 1279.

10. A. S. Toporets, "Study of Diffuse Reflection from Powders Under Diffuse Illumination," Optics and Spectroscopy, Vol. 7, 1959, p. 471.

11. A. C. Hardy and D. W. Pineo, "Errors Due to Finite Size of Holes and Sample in Integrating Spheres," Journal of the Optical Society of America, Vol. 21, 1931, p. 502.

12. J. P. Dawson, D. C. Todd, B. E. Wood, et al., "Deviations from Integrating Sphere Theory Caused by Centrally Located Samples," AEDC-TR-65-271, 1966.

13. J. P. Dawson, B. A. McCullough, B. E. Wood, and R. C. Birkebak, "Thermal Radiative Properties of Carbon Dioxide Cryodeposits," Paper presented at the Sixth Annual Symposium on Space Environmental Simulation, May 1965.

14. K. E. Torrance, E. M. Sparrow, and R. C. Birkebak, "Polarization, Directional Distribution, and Off-Specular Peak Phenomena in Light Reflected from Roughened Surfaces," Journal of the Optical Society of America, Vol. 56, 1966, p. 916.

15. P. A. Tellex and J. R. Waldron, "Reflectance of Magnesium Oxide," Journal of the Optical Society of America, Vol. 45, 1955, p. 19.

16. W. Budde, "Standards of Reflectance," Journal of the Optical Society of America, Vol. 50, 1960, p. 217.

17. B. P. Kozyrev and O. E. Vershinin, "Determination of Spectral Coefficients of Diffuse Reflection of Infrared Radiation from Blackened Surfaces," Optics and Spectroscopy, Vol. 6, No. 4, 1959, p. 345.

18. E. R. G. Eckert and R. M. Drake, Jr., Heat and Mass Transfer, McGraw-Hill Book Company, Inc., 1959, p. 372.

19. G. A. Zerlaut and A. C. Krupnick, "An Integrating-Sphere Reflectometer for the Determination of Absolute Hemispherical Spectral Reflectance," AIAA Journal, Vol. 4, No. 7, 1966, p. 1227.

20. W. M. Brandenberg, "The Reflectivity of Solids at Grazing Angles," NASA SP-31, Measurement of Thermal Radiation Properties of Solids, 1963, p. 75.